

# A force-flow oriented segmentation strategy of standard veneer plates for non-standard superlamellas

A “roadmap” for digitally assisted fabrication of veneer-reinforced timber structures

Master Thesis  
Department of Architecture  
TUM School of Engineering and Design  
Technical University of Munich

**Supervised by** Prof. Dr. sc. ETH Kathrin Dörfler, Iuliia Larikova  
TT Professorship of Digital Fabrication

Niklas Kainz  
Lehrstuhl für Holzbau und Baukonstruktion

**Submitted by** Zhan Shi  
Munich, 11.09.2023

# Abstract

A novel veneer-reinforced timber product for load-bearing applications has been explored and developed on the background of climate change, motivated by the need for renewable resources and low-carbon solutions in the construction industry. Veneer plates with custom layer orientation, also known as superlamellas, are inserted into a glulam cross-section to reinforce shear and tensile stresses perpendicular to the grain for this composite timber product. This thesis investigates the utilization of segmented standard veneer plates joining together to produce non-standard superlamellas as a digitally informed fabrication approach for user-defined load cases.

A segmentation strategy for this customized veneer structure is inspired by cellular division in the natural world, utilizing the weighted average orientations of the internal force flow to drive the subdivision of entities within the respective glulam beams. The geometries of segments are then detailed with timber joints into milling paths with orientations following the internal stress directions. These segments are packed and nested on the milling material to minimize the waste of veneer plates. The segmented veneer plate pieces are assembled and inserted to create the superlamella-reinforced timber beams. A compact design tool is developed on the parametric software platform and utilized to generate the milling paths for fabricating beam fragments as two prototypes built on the scale of 1:5.

This thesis presents an innovative approach to fabricating the load case customized superlamellas for veneer-reinforced timber structures, merging computational design and modeling methods with practical digitally assisted fabrication. Future collaborations with industry partners promise further refinement and practical application of the scenarios explored herein, potentially revolutionizing veneer product fabrication.

# Kurzzusammenfassung

Vor dem Hintergrund des Klimawandels und motiviert durch den Bedarf an erneuerbaren Ressourcen und kohlenstoffarmen Lösungen in der Bauindustrie wurde ein neuartiges furnierbewehrtes Holz für tragende Anwendungen erforscht und entwickelt. Bei diesem Holzprodukt werden in einen Querschnitt der Brettschichtholz Furnierplatten mit individueller Faserorientierung, auch Superlamellen genannt, zur Verstärkung von Scher- und Zugspannungen senkrecht zur Belastung eingesetzt. In dieser Arbeit wird die Verwendung von segmentierten Standardfurnierplatten untersucht, die miteinander verbunden werden, um nicht standardisierte Superlamellen als digital informierten Herstellungsansatz für benutzerdefinierte Lastfälle zu erzeugen.

Eine Segmentierungsstrategie für diese individuelle Furnierstruktur ist von der Zellteilung in der Natur inspiriert und nutzt die gewichteten durchschnittlichen Orientierungen des internen Kräfteverlaufs, um die Unterteilung der Einheiten innerhalb der jeweiligen Brettschichtholzträger zu steuern. Die Geometrien der Segmente werden dann mit Holzverbindungen in Fräswege detailliert, deren Orientierungen den inneren Spannungsrichtungen folgen. Diese Segmente werden auf dem Fräsmaterial verschachtelt, um den Verschnitt an Furnierplatten zu minimieren. Die Teile werden dann zusammengesetzt und eingefügt, um die superlamellenbewehrten Holzbalken zu erstellen. Ein kompaktes Designwerkzeug wird auf der parametrischen Softwareplattform entwickelt und zur Generierung der Fräswege für die Herstellung von Balkenfragmenten als zwei Prototypen im Maßstab 1:5 verwendet.

In dieser Arbeit wird ein innovativer Ansatz zur Herstellung von individuellen Superlamellen für furnierbewehrte Holzkonstruktionen vorgestellt, der computergestützte Entwurfs- und Modellierungsmethoden mit praktischer, digital unterstützter Fertigung verbindet. Zukünftige Kooperationen mit Industriepartnern versprechen eine weitere Verfeinerung und praktische Anwendung der hier untersuchten Szenarien und könnten die Herstellung von Furnierprodukten revolutionieren.

## List of Abbreviations

CNC -- Computer numerical control

Brep -- Boundary representation

LVL -- Laminated veneer lumber

LVL-P -- Laminated veneer lumber with parallel bonded veneers

LVL-C -- Laminated veneer lumber with cross-bonded veneers

GLT -- Glued laminated timber

VRT -- Veneer-reinforced timber



# Glossary

**CNC:** Computer numerical control, an automated control of machining utilizing a computer.

**CNC milling:** A machining process that employs computerized controls and rotating multi-point cutting tools to progressively remove material from the workpiece and produce a custom-designed part or product.

**Parametric design:** A process based on an algorithmic approach that expresses parameters and rules that can define, encode, and clarify the relationship between designer's intent and design response.

**Digitally assisted fabrication:** A manufacturing process where a computer controls a machine.

**Veneer-reinforced timber:** A composite timber product, in which veneers are inserted vertically to the cross-section of glued laminated timber to reinforce shear and tensile stresses perpendicular to the grain in veneer-reinforced timber.

**Superlamella:** Veneers with a custom arrangement of the veneer fiber directions at angles between 0° and 90°.

**Standard superlamella:** A superlamella with a constant fiber arrangement on each customized load case.

**Non-standard superlamella:** A superlamella that is freely formed in fiber orientations and individually tailored to structures on each customized load case.

**Fiber orientation:** The arrangement of veneer fibers in the veneer-reinforced timber composite.

**Finger joint:** A woodworking joint made by cutting a set of complementary, interlocking profiles in timber elements.

**Scarf joint:** An woodworking overlap joint where the contacting angle of the two members is more than 0° and less than 90°.

# Table of Contents

List of Abbreviations.....	4
Glossary .....	5
1. Introduction.....	8
1.1. Motivation .....	8
1.2. Research Ideas .....	9
1.3. Aims and Objectives .....	12
1.4. Methods.....	13
2. State of the Art.....	15
2.1. Digital Design .....	15
2.1.1. Force-flow Oriented Design.....	15
2.1.2. Tessellation and Biomimetic.....	17
2.1.3. Nesting in Manufacturing.....	18
2.2. Veneer Wood Products.....	19
3. Design Tool Modeling .....	22
3.1. Design Tool Concept and Structure .....	22
3.2. Analysis of Input Files .....	23
3.3. Segmentation Based on Cellular Division Process.....	26
3.3.1. Definition of Cell.....	26
3.3.2. Subdividing Process.....	28
3.3.3. Multilayering and Staggered Seams.....	30
3.3.4. Structural Refinery after Segmentations.....	32
3.4. Joints Generation.....	33
3.4.1. Neighbouring Finding .....	33
3.4.2. Finger Joint Generation.....	34
3.4.3. Scarf Joint Generation .....	35
3.5. Nesting and Final Milling Paths.....	37
3.6. Interface Design and Assembly Display .....	40
4. Use Case Study – Segmented Timber Beams .....	43
4.1. Use Cases .....	43
4.2. Setup on Digital Cutter.....	47
4.3. Veneer Milling Process .....	49
5. Results .....	51
5.1. Summary.....	51

5.2.	Fabrication of Prototypes .....	53
5.3.	Milling with the Digital Cutter.....	55
6.	Conclusion .....	60
6.1.	Discussion .....	60
6.2.	Future Work.....	61
7.	Bibliography.....	63
8.	List of Figures .....	66
9.	List of Tables .....	70

# 1. Introduction

## 1.1. Motivation

On the background of climate change, the need for renewable resources and low-carbon solutions has never been more acute. The building industry contributes crucially to carbon emissions, thereby exacerbating climate change. In Germany, resources have been allocated significantly towards the construction industry. The utilization of mineral raw materials is at 90% producing building materials and products, and the building sector accounts for about 40% of total greenhouse gas emissions in Germany (Graf et al., 2022). With a long tradition in the construction industry, timber offers a renewable alternative to other materials like concrete and steel. It has a low carbon footprint and acts as a carbon sink, storing carbon dioxide throughout its lifecycle. As the urgency for climate action gains momentum, using sustainable materials like wood becomes indispensable.

Consequently, the Ministry of Food and Agriculture has outlined a strategic agenda named Charter for Wood 2.0 to augment the utilization of wooden resources within the nation's construction (Graf et al., 2022). A well-known characteristic of timber products is its anisotropy due to its unique cell structure. For instance, its tensile strength, when measured in the fiber direction, is approximately double that measured perpendicular to it (Wittchen et al., 2006). Moreover, the compressive strength across the fiber has 10 to 15% of the strength in the fiber direction (Wittchen et al., 2006). This distinct variation emphasizes the importance of considering the correct fiber orientation in construction to bolster the structural integrity of the timber.

The German government has brought the national strategic initiative of Industry 4.0, aiming at resource productivity and efficiency (Kagermann et al., 2013). Construction processes integrate computational design and digitally assisted fabrication methods, reinventing the traditional material use and labor paradigms. These advancements have relevance for timber construction,

allowing for shorter manual construction times on site and more structurally efficient utilization of material resources. Moreover, digital design tools empower architects and engineers to achieve structural and spatial integrity while enabling designs to be easily reconfigured for varying tasks or adapted to site-specific conditions. Combining digital design with computer numerical control milling allows the fabrication of timber structures with great customization and accuracy, making it feasible to construct complex geometries that cater to the unique needs of each project. Figure 1 captures a plywood CNC milling project of great geometrical complexity. We can capitalize on the timber's material strengths by strategically aligning the fiber direction with their internal force distribution in digital design and fabrication.



Figure 1: The interior renovation project was nested onto 1200 3.6m \* 1.2 m plywood sheets and milled using a small 3-axis CNC router, *dECOi Architects*.

## 1.2. Research Ideas

With the purpose of improving the structural behavior of timber for load-bearing applications, the Chair of Timber Structures and Building Construction of the

Technical University of Munich conducts a research project on veneer-reinforced timber, which is a new type of composite timber product (Lechner et al., 2021). In the fabrication of this product, hardwood veneers are inserted vertically to the cross-section of a glued laminated timber (glulam) for local reinforcement (Fig. 2). As a result, the highly anisotropic strength and stiffness properties of glulam are homogenized, resulting in a new, high-performance timber construction product (Lechner et al., 2021). Chapter 2 State of the Art presents a more detailed analysis of veneer-reinforced timber projects and present fabrication.

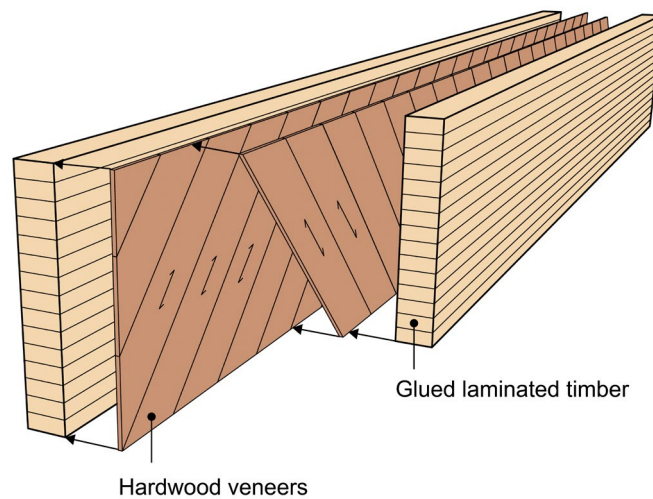


Figure 2: Principal structure of veneer-reinforced timber, Markus Lechner.

Opposed to standard veneer-reinforced timber with orthogonal layer orientation as veneer reinforcement, in this non-standard superlamellas, the arrangement of veneer layers between the glulam components varies at angles from  $0^\circ$  to  $90^\circ$  responding to the internal stresses. Figure 3 shows a possible arrangement of veneers for non-standard superlamellas in a pitched cambered beam.

Individual fiber layouts can take advantage of heterogeneity in the veneer plate, strengthening the outcome structural behavior.

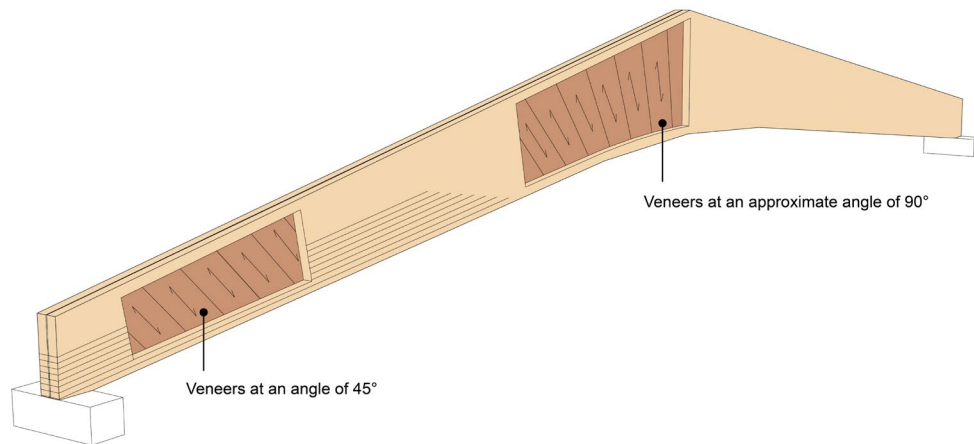


Figure 3: A possible arrangement of veneer for non-standard superlamella in pitched cambered beam, Markus Lechner.

To further improve the structural properties of veneer-reinforced timber, this master thesis researches a new design and fabrication solution, focusing on fabricating the force-flow oriented segmented superlamella beam via computer numerical control milling, also known as CNC milling. This research aims to develop a computational strategy for controlling veneer fiber's direction on every segment and generating milling paths for customized superlamellas based on given load-bearing cases. Parametrical design methods and advancements in construction technologies facilitate the fabrication of complex and customized geometries and the creation of data-driven design paradigms capable of considering multiple input parameters. Therefore, the central idea of the present research is to create a digital road map for fabricating force-flow oriented, segmented, and non-standard superlamella beams with standard laminated veneer plates, reacting to internal load distribution of structure, optimizing veneer layer geometry for minimal resource expenditure.

### 1.3. Aims and Objectives

The research objective of this project is to explore the veneer material and develop a segmentation strategy for standard lamella plates to create non-standard superlamella structures, which will be inserted in veneer-reinforced timber as reinforcement. Given the limited time frame of a master's thesis, the research focuses mainly on examining the utility of computational design and digitally assisted fabrication in creating non-standard superlamella beams. The research goals of this thesis are summarized by the following objectives in Figure 4:

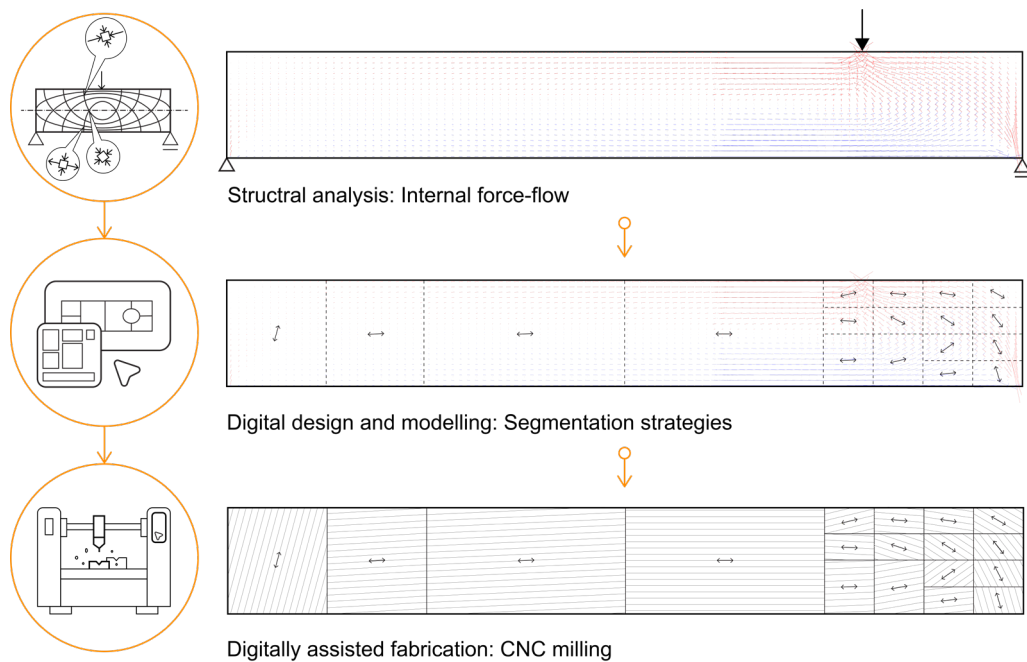


Figure 4: Research objectives.

- Adopting a force-flow oriented strategy for segmenting beam structures: By arranging the structure segments in alignment with the inherent flow of forces, this objective seeks to strengthen the structural behavior.



- Generating timber joints for the segments: Timber joints facilitate easy assembly and secure connections between components. This objective is crucial for enhancing the overall integrity and stability of the constructed structures.
- Nesting geometries on veneer plates: By optimizing the spatial layout of the segments, the research intends to minimize waste and promote efficient utilization of material resources.
- Developing a user-friendly design tool: The design tool is acutely aware of all input parameters, enabling a more adaptive and flexible design process for fabricating the non-standard superlamella beam.
- Fabricating a final mock-up by CNC milling methods: A final fabrication of distinct non-standard superlamellas validates the design tool's solutions.

## 1.4. Methods

The methodology adopted in this thesis is a blend of theoretical, computational, and experimental techniques to further the comprehension and application of digital design and fabrication, with a focus on veneer products.

Analyses of reference projects on a building scale that deal with digital design and fabrication of veneer products, together with a literature review, are used to contextualize this thesis in State-of-the-Art research and define a design and research approaches that allow the basis of design studies on theoretical ground. The review explores the research papers and doctoral theses in the field. As the feed-in data for this thesis, the structural analysis results come

from the structure analysis software *SOFiSTiK*, which provides structural engineering analyses with finite element analysis.

The Design Tool Simulation takes place on the quite common 3D modeling software *Rhinoceros 7.0* in conjunction with the parametric modeling environment *Grasshopper* and the programming language *Python 2.7* (Fig. 5). Both Rhino and Grasshopper are used prevalently in the fields of architecture and construction. The Python code is written based on the *Rhino.Python* framework inside *IronPython*. Two additional plugins on the platform *Grasshopper* are integrated into the design tool: *OpenNest 1.5.1* and *UiPlus 1.9.3*. The plugin *OpenNest* is employed for arranging the geometries on milling veneer sheets, while *UiPlus* enhances the user interface within *Grasshopper*.

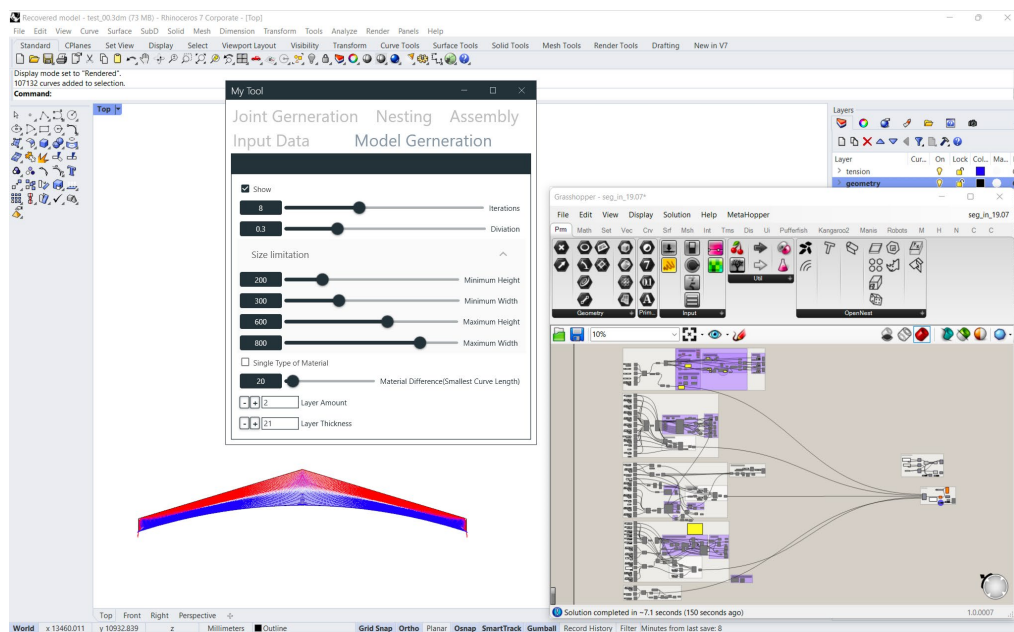


Figure 5: Software platform.

To verify the feasibility of the fabrication process, the author conducted two prototyping experiments on a 1:5 scale with a Zünd G3 flatbed digital cutter at the Technical University of Munich mills the geometrical solutions with standard laminated veneer plate.

## 2. State of the Art

With the goal of contextualizing the project, I analyze existing State-of-the-art projects and research and divide these into two thematic chapters: Digital Design and Veneer Products Fabrication.

### 2.1. Digital Design

#### 2.1.1. Force-flow Oriented Design

Improving the performance of a structure is a primary purpose of structural design and optimization. Digital fabrication strategies, such as Additive Manufacturing, allow for the labor and resource-efficient production of structure-aware designs. For example, an MIT-based research group has presented an innovative design-to-fabrication workflow for additive manufacturing, adding material explicitly along the three-dimensional principal stress lines of shell structure (Tam et al., 2017)(Fig. 6). Connecting load-bearing status and application of material in the planning extends limits of the system. It allows for resource-efficient production of building elements, where material is only placed where it is functionally needed.



Figure 6: The resulting specimens, Kam-Ming Mark Tam and Caitlin Mueller.

Not only does the solid material extrusion build up the optimized geometries, but the fiber arrangement reinforcing material can also be adapted based on its force-flow orientation. German researchers apply continuous fibers to 3D-printed plastic parts, enhancing mechanical properties (Heitkamp et al., 2022). Fibers are embedded along the principal stress trajectories in a load-oriented manner instead of regular patterns without utilizing their outstanding strength and stiffness properties (Fig. 7). It has been proven in the tensile and flexural tests that optimized layouts of carbon fibers on polyamide specimens behave with a significant increment in the strength of the additively manufactured parts (Heitkamp et al., 2022).

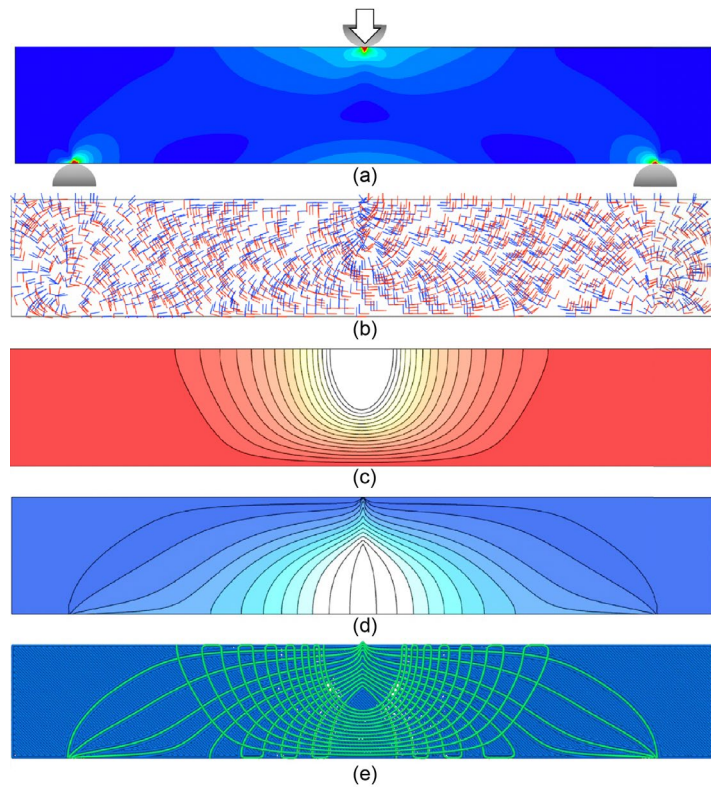


Figure 7: Exemplary process flow for generating a stress-adapted infill pattern. (a) Setup for structural analysis. (b) calculation of the principal stresses. (c) Compressive stress trajectories. (d) Compressive stress trajectories. (e) G-code for fabrication. Tim Heitkamp.

### 2.1.2. Tessellation and Biomimetic

Tessellation is covering a surface using one or more geometric shapes without overlapping or gaps (Kizilörenli et al., 2021). With the help of digital fabrication, designers can approximate complex geometries with irregular patterns in architectural projects. One of the examples is the Landesgartenschau Exhibition Hall from the University of Stuttgart. The polygonal planar plate penalization approximates the double-curved timber shell structure, resulting in 367 geometrically unique elements of hexagonal shape (Wagner et al., 2020). The hollow LVL segments with finger joints are individually prefabricated through a CNC milling machine and assembled by industrial robots. The fiber grain direction of the top and bottom plates of the timber components are aligned with the global force flow in the structure, for the best use of material (Fig. 8).

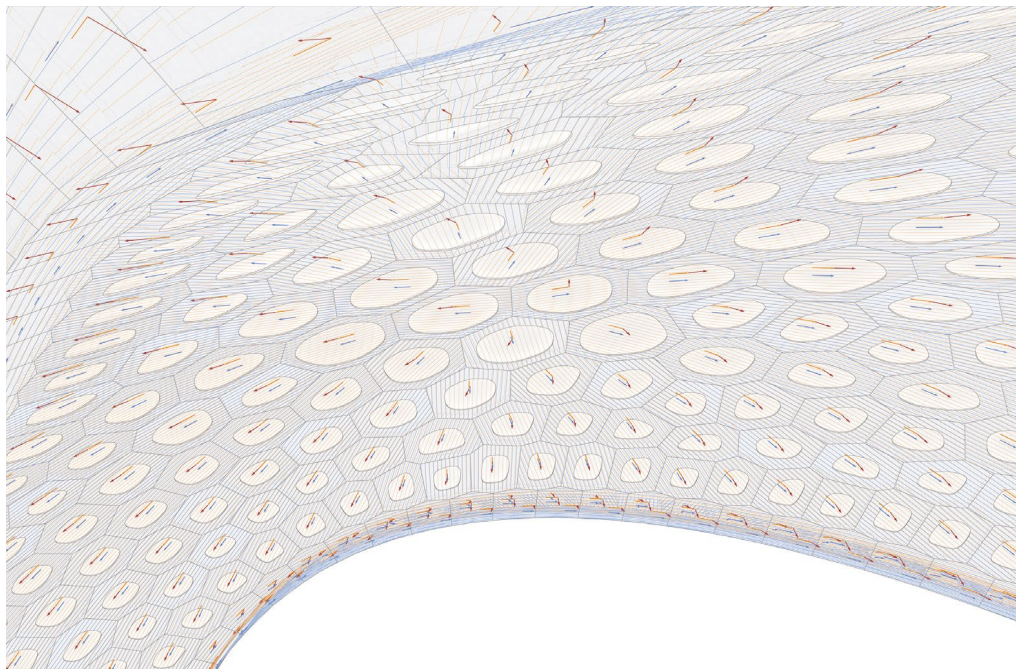


Figure 8: Interior of the building demonstrator, ICD/ITKE University of Stuttgart.

In the manner that Stuttgart's project follows the principles found in the plate skeleton of sea urchins (Sonntag et al., 2019), the concept of biomimetics is



utilized widely in architectural design. Designers follow the biological rules found in the natural world and interpret them with new aesthetical and functional creations. A built project in Beijing utilized cellular growth simulations by a designer from the University of Cincinnati (Klemmt et al., 2020). The unique geometry of the indoor installation comes from the algorithm articulating and adjusting local behaviors of cells and external forces (Figure 9) (Klemmt et al., 2020).



Figure 9: Photo of Gaizoshoku in the Lobby, Christoph Klemmt.

### 2.1.3. Nesting in Manufacturing

In the current manufacturing industry, cutting two-dimensional shapes from standard sheets while minimizing material wastage is a common task known as nesting. In the sheet metal industry, nesting algorithms are mature, with evolutionary algorithms being one of the more prevalent methods for handling these problems (S.V.Berg et al., 2022). One of the recent studies is nesting dealing with constraints of flatbed laser-cutting machines from Karlsruhe Institute of Technology. The researchers implemented a nesting algorithm as an evolutionary algorithm. They added additional limitations considering the laser-cutting machine, such as margins around parts and gas-pressure points influencing the cut part (Struckmeier et al., 2019). Aside from the research field, the nesting function is applied to the *Zünd G3 XL-1600* digital software platform

at the Technical University of Munich to optimize raw material utilization (Zünd Systemtechnik AG, 2020).

## 2.2. Veneer Wood Products

A veneer is a sheet of wood obtained by peeling, slicing, or sawing from the tree trunk or its root. The industry divides them into three groups according to their manufacturing process: sawn veneers, sliced veneers, and peeled veneers (Fritz Kohl GmbH & Co. KG, 2017). One of the most common mass products is laminated veneer lumber (short as LVL). These LVL boards are produced from 3mm bis maximal 6 mm thick veneers and bonded together with an adhesive (DIN EN 14279, 2009). Depending on the grain orientation, two variations of this product are available in most manufacturing companies: LVL-P, which consists of veneers with grains running parallel to each other, and LVL-C, where some layers of veneers are oriented cross-grain.

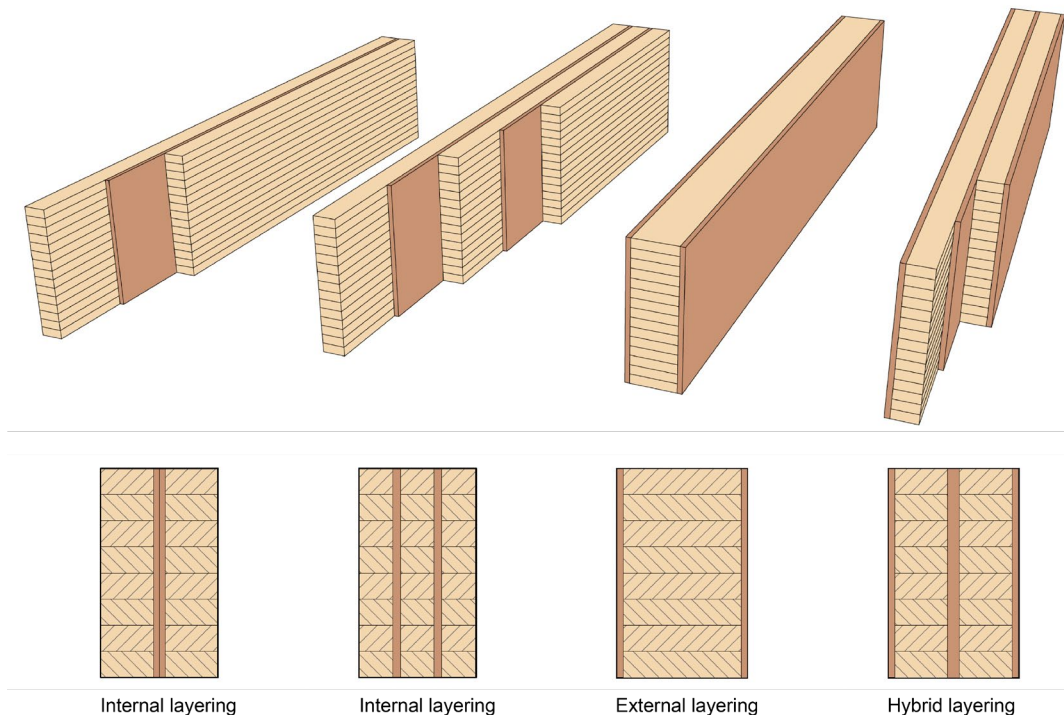


Figure 10: Possible arrangements of veneers in VRT, Markus Lechner.

To improve the strength and stiffness of the glued laminated timber, the researchers from the Technical University of Munich insert hardwood veneers as local deformation-compatible reinforcements for the structure, usually perpendicular to the grain direction of the wood component (Lechner et al., 2021). The veneer layers plate consists of one or more layers laminated on each other. The veneer plates or superlamellas can be arranged once or multiple times onto the interior or exterior of GLT (Fig. 10) (Lechner, 2020, 2021). This novel timber structure is called veneer-reinforced timber.

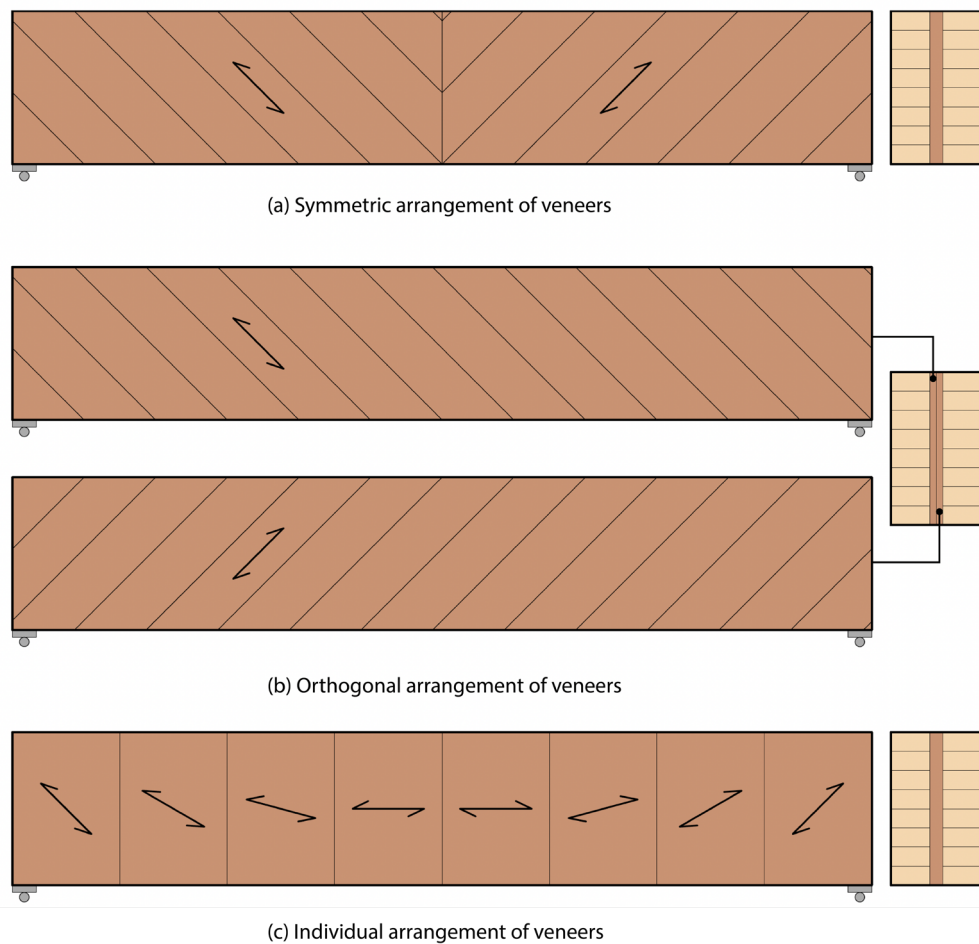


Figure 11: Veneer arrangements in VRT, Markus Lechner.

In contrast to conventional laminated veneer lumber, the veneer layers in so-called superlamella are not glued orthogonally but with a custom arrangement of the veneer fiber directions at angles between  $0^\circ$  and  $90^\circ$ . Non-standard



superlamellas are freely formed in fiber orientations and individually tailored to structures on each customized load case. In contrast, “standard” ones with a constant design can be massively produced utilizing established methods (Lechner, 2021)(Fig. 11).

In the project of veneer-reinforced timber, researchers glued veneer strips together to build up the veneer reinforcements. They design different orientations of the veneer fibers for experimental validation via mechanical tests (Lechner, 2021). Depending on the inclination angle, single-layered veneer strips are then cut at an angle to minimize waste. Figure 12 illustrates the basic manual production process of the veneer strips (Lechner, 2021). In this thesis, the orientation of veneer fiber in the superlamellas varies in reactions to different load cases. Instead of manually gluing the strips, the veneer reinforcement components will be milled and assembled from standard LVL plates.

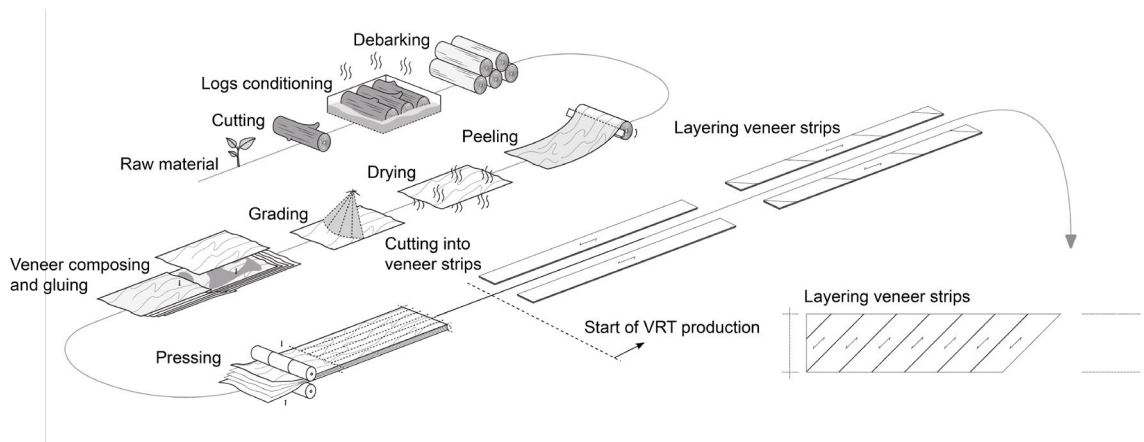


Figure 12: Production of veneer strips glued parallel to the fibers as a preliminary product to produce veneer-reinforced timber, Lechner Markus.

## 3. Design Tool Modeling

### 3.1. Design Tool Concept and Structure

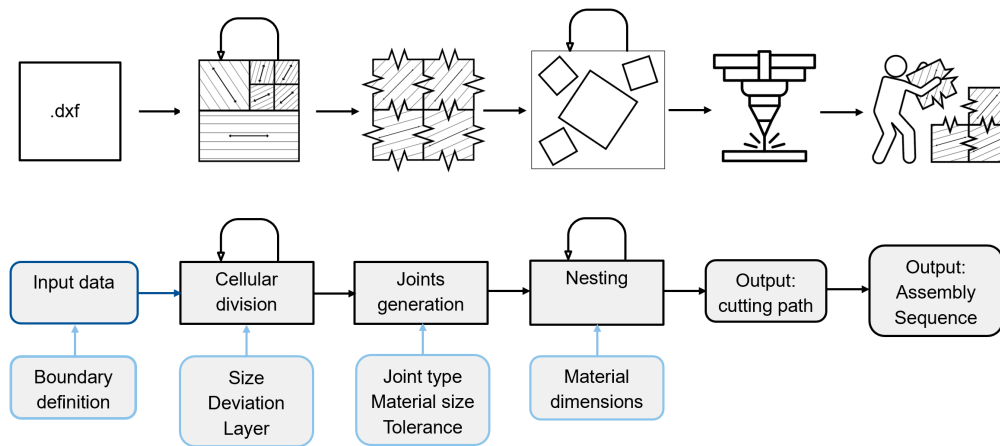


Figure 13: Workflow of the design tool.

As mentioned in previous chapters, this design tool is developed under the awareness of the fabrication method by CNC milling and delineated into five distinct components:

- The parsing and filtration of structural analysis from input files.
- The segmentation of input geometry in reaction to its internal force distribution.
- The generation of timber joints for the segments.
- The efficient arrangement and nesting of these segments for the final CNC milling.
- The visualization of a coherent assembly sequence.

Figure 13 illustrates the overall workflow of the design tool. This structure shows a 'bottom-up' design concept, originating from the foundational and

simple geometry components, gradually assembling them into a coherent and functional whole.

*Python 2.7* has been adopted as the programming language for the tool, utilizing the *RhinoCommon* library to execute essential geometric operations. Regarding object-oriented programming, the author structures the code into two Python classes: "Cell" and "Plate". The following objects will be named without double quotes in this thesis. These classes manage the cellular division of structures and establish interconnections among the divided elements. The tool also integrates complementary functions to ease the generation of joints. Future sections will elaborate on this aspect.

A prominent aspect of this approach centers on the transformation of intricating three-dimensional geometries into instances of these classes, thereby enabling the attachment of additional information to each entity. In addition to geometric attributes, a cell instance encompasses an array of data, including the weighted average of internal forces within the cell's confines, the position of the cell within the assembly hierarchy, its status requiring further subdivision, and various other distinctive characteristics. These attributes are computed during object instantiation and remain accessible as variables. An advantage of incorporating this stratum of information during the transformation from three-dimensional boundaries to instances is the acceleration during model operations. The tool can execute joint geometry manipulations without requiring a comprehensive recomputation of all topological data. The foundational data structure, established during the initial conversion of the 3D model into discrete class instances, already incorporates these particulars.

## 3.2. Analysis of Input Files

Our engineering researcher exports the exchange files from the structure analysis software *SOFiSTiK*, which provides structural engineering analyses with finite element analysis. The resultant data of a beam are the geometrical

boundary, the loads and supports, the principal stresses' directions, and their values. The *.dxf* format encapsulates the data, short for Drawing Exchange Format or Drawing Interchange Format. *Rhinoceros 7.0* software lacks vector format as a geometry type, so it displays the given internal tensile and compressive stresses as lines. The beam structure has an automatically generated mesh, with the force lines for each face (Fig. 14, left). These lines' lengths are proportionally related to their stress values. Upon data transfer, the ensuing step involves utilizing the *Grasshopper* platform to facilitate the conversion of these lines into vector representations (Fig. 14, right), allowing for further analysis within the chosen software platform.

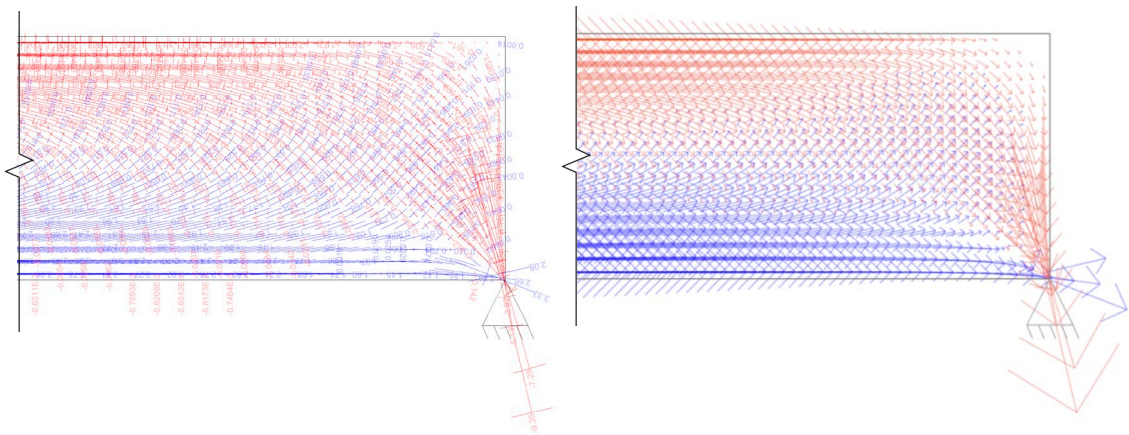


Figure 14: Part of the input file of a rectangular beam in *Rhinoceros 7.0* (left), the same part after data filtering in *Grasshopper* (right).

Two primary challenges have surfaced within the dataset. Firstly, some data lines are too short, potentially leading to computational redundancy in further analysis. Secondly, both ends of the data lines representing compression retain unnecessary and inaccurate dimension marks. In order to enhance the overall reliability of the dataset, an additional data filtering approach has been developed. The suggested solution involves applying a length-based filter, followed by an evaluation of line positioning, which involves calculating the distance between a line's midpoint and the endpoints of other lines. By comparing this distance to a predetermined tolerance, instances indicating dimension marks can be accurately identified and removed from the dataset (Fig. 15). This filtering process in the design tool is expected to resolve most of such anomalies effectively.

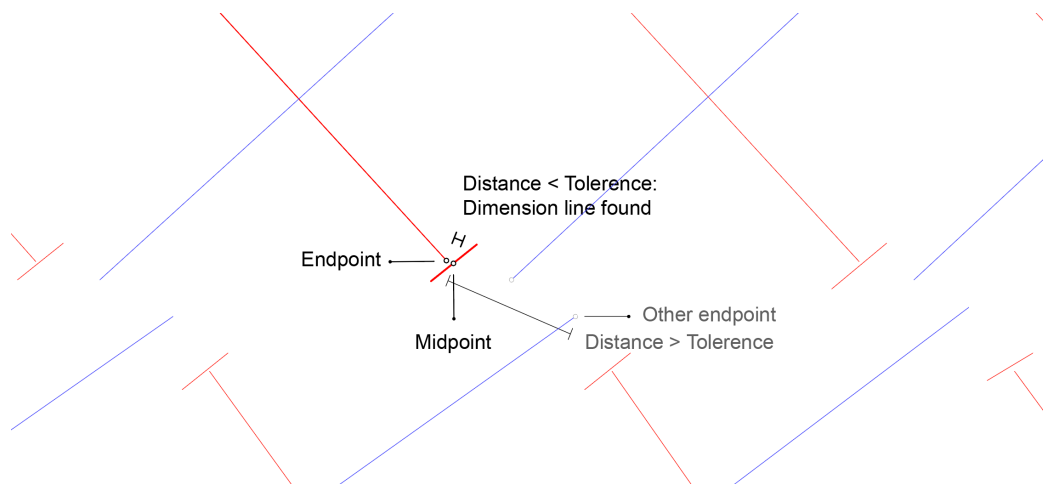


Figure 15: A principal sketch on finding dimension lines on a zoomed-in of input data.

For the remaining cases, a practical approach involves incorporating a weighted average methodology when calculating the average orientation. Figure 16 shows that after filtering, *Grasshopper* receives the input data from the structural analysis of various beams into the tool for further calculation, in dispute of the amount of data and their locations. To simplify the data feed-in process, users can select all the lines representing forces and a geometrical boundary under the “Input Data” tab in the user interface. The tolerance value for filtering is modifiable as the length of lines. The input of boundary can be adaptable to much more complex geometries than a rectangular beam in Figure 16(a). For example, 16(b) is rectangular beam a circular cutout and (c) is a pitched cambered beam.

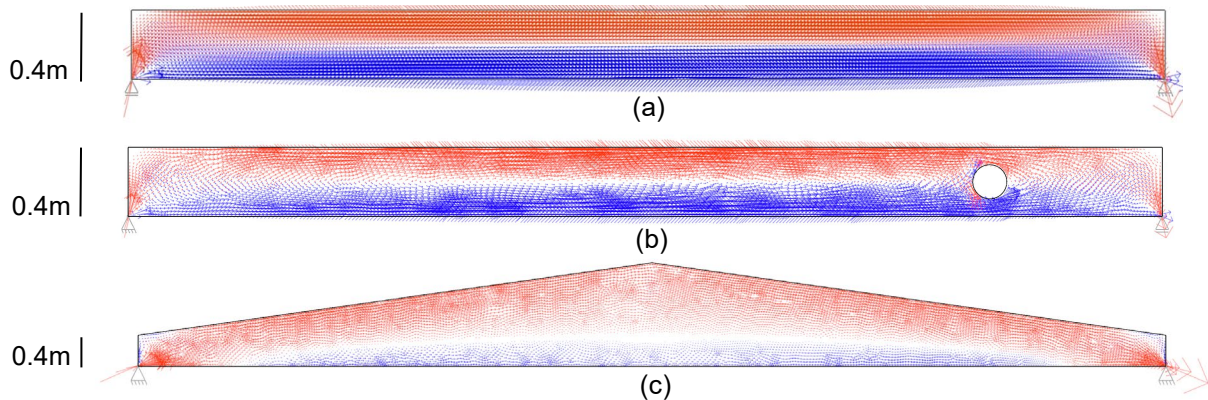


Figure 16: Vector results in *Grasshopper* after data filtering.

### 3.3. Segmentation Based on Cellular Division Process

#### 3.3.1. Definition of Cell

The segmentation strategy draws inspiration from the cellular division process in the natural world. This conceptualization defines a cell entity in *Python 2.7* class by its spatial boundary, represented as *Brep* in *Rhinoceros 7.0* environment. The script does not apply joints to its geometry at this stage yet.

The user-defined structure sets the geometric boundary for the initial cell. These cells possess dynamic states of either "splitting" as they will divide in the next iteration or "stable" when fully formed (Fig. 17). Like biological cells store genetic information, each cell will store the weighted average of internal force vectors as their information. After every entity in the system finishes a state assessment and a subsequent action, an iteration completes, and all the cells initiate the next hoop.

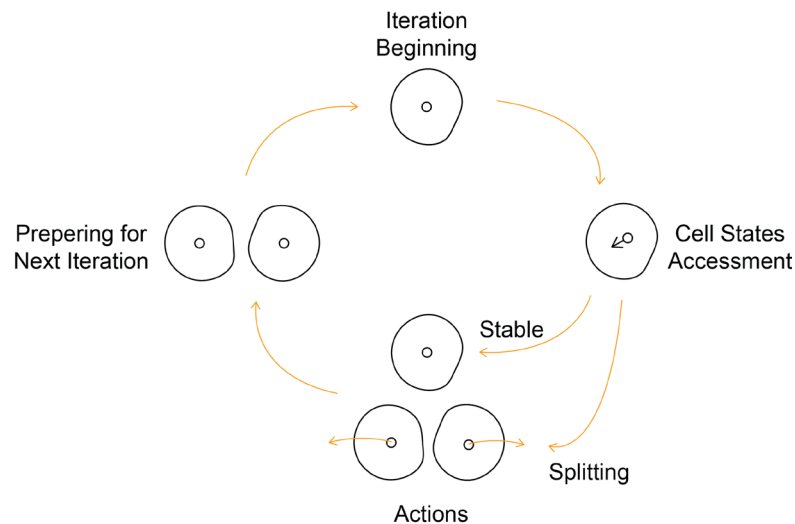


Figure 17: Concept of the cellular division modeling.

When defining a new cell, the function *computeVector()* calculates its tensile and compressive force vectors separately and stores the outcome as separate

object attributes. If these two vectors exceed the customized input value, the function *getForce()* will summarize them when presenting the results. The calculations in *computeVector()* are:

$$\text{Sum Vector} = \text{Vector} + \text{previous Sum Vector}$$

$$\text{Sum Length} = \text{Vector Length} + \text{previous Sum Length}$$

$$\text{Vector Result} = \frac{\text{Sum Vector}}{\text{Sum Length}}$$

The "splitting condition" serves as a crucial determinant for the division of cells. In this modeling process, two key factors define the splitting condition: the summary of deviation between the internal forces within a cell and its weighted average, alongside the limitations imposed on the dimensions as set by the user. These dual constraints ensure that internal force deviation within their region and customized component dimensions for fabrication influence cell divisions. When internal forces within a cell deviate from their weighted average, it indicates a distinguishable deviation in stress distribution within this boundary. Figure 18 is a flowchart of a cell evaluation process:

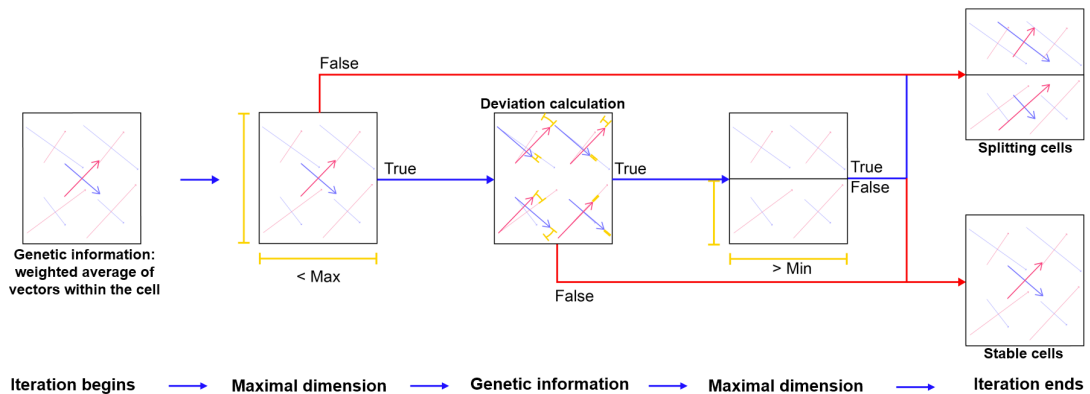


Figure 18: Cell state definition constraints on one iteration

Different sizes of cells indicate their orientations at variance, as shown in Figure 19. The splitting condition triggers the splitting process, decreasing the weighted average internal force direction difference. At the same time, user-

specified element size constraints gain an additional layer of control, fine-tuning the segmentation process to fulfill both structure and design intent.

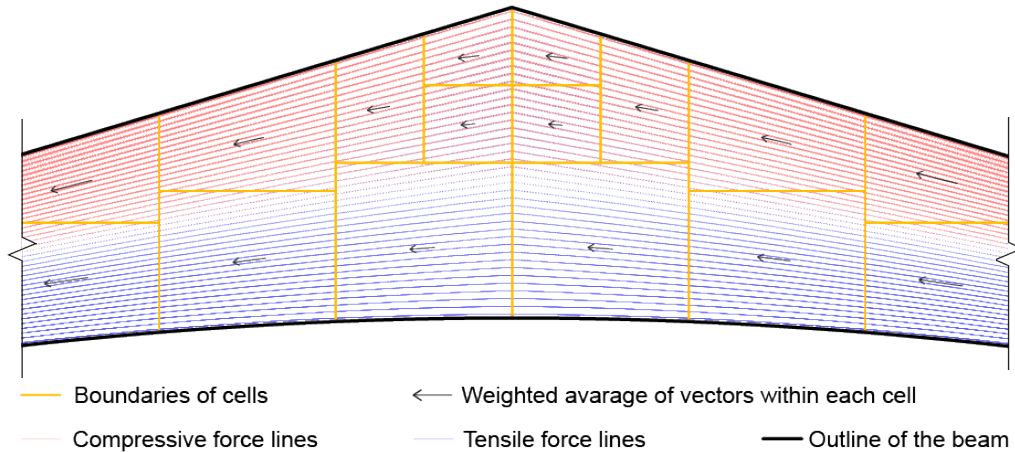


Figure 19: Different sizes of "cells" with their weighted average vectors compared to the input data for a pitched cambered beam.

### 3.3.2. Subdividing Process

The subdivision iteration involves a systematic approach to achieve limited component dimensions and generate internal stress orientation. The input parameters include the desired dimensions for the final segments and an allowable deviation in internal force orientation within each cell region. If a cell is within the range of dimension limitation, the subdivision of entities will begin.

The Boolean Split from RhinoCommon calculates for the splitting. Figure 20 outlines this procedure. A bounding box passing through the midpoint of a cell's longest edge is drawn vertically or horizontally and perpendicular to this edge. This simple rectangular volume can simplify the Boolean function, and the splitting direction enhances controllability during the subdivision process. After subdivision, the procedure entails the creation of two new cells from the split Brep, followed by the computation of each weighted average of internal forces within these cells. If the iteration reaches its target or all cells in the system are



"stable", the subdivision procedure will determine. The resultant orientation of internal forces decides the direction of each cell segment for the afterward milling.

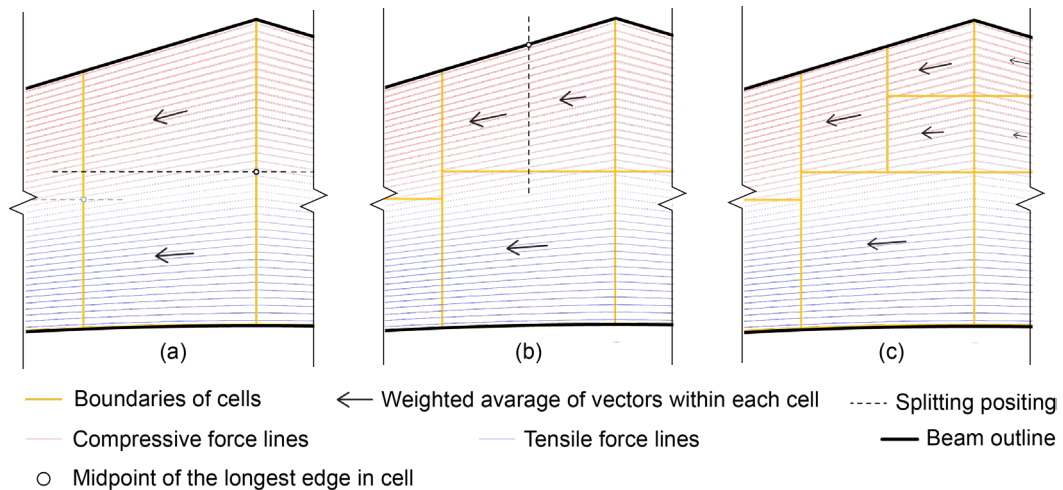


Figure 20: Cell subdivision (a) horizontally and (b) vertically, cells after subdivision (c) compared to the input data for a pitched cambered beam.

After modeling the segments, users can define the summarization manners for different milling materials. There are extra inputs for users to define the types and thickness of veneer plates and how to summarize the tensile and compressive stress orientation. When dealing with one kind of veneer, the resultant compressive and tensile vector summary decides the plate orientation. When dealing with both cross and parallel-bonded veneer plates, a summarization of vectors becomes pivotal. The assessment involves comparing a smaller vector to the input parameter. If the vector length surpasses the input, the material classification becomes "C", indicating that the veneer plate is bonded in a cross orientation. In this case, the resultant vector is the addition of compressive and tensile vectors. If the summarization remains within the boundaries of the input values, the material is denoted as "P," signifying a parallel glued veneer plate. The resultant vector only takes the value of a more significant force vector. This methodology optimizes the segments' veneer orientations for diverse loading scenarios.

### 3.3.3. Multilayering and Staggered Seams

In the veneer-reinforced timber project, multiple layers of veneer plates can be added to the structure. In the prototype experiments described in chapter 4 of this thesis, standard LVL boards for milling are laminated with at least five layers of veneer for construction in Germany (DIN 14374, 2009). Regardless, the joinery of timber segments could still be weak on the structure. Therefore, implementing multiple LVL boards with staggered seams might be practical in enhancement. This approach ensures the cells' segmentation in different positions and the disconnection of load distribution spreads across the composite material.

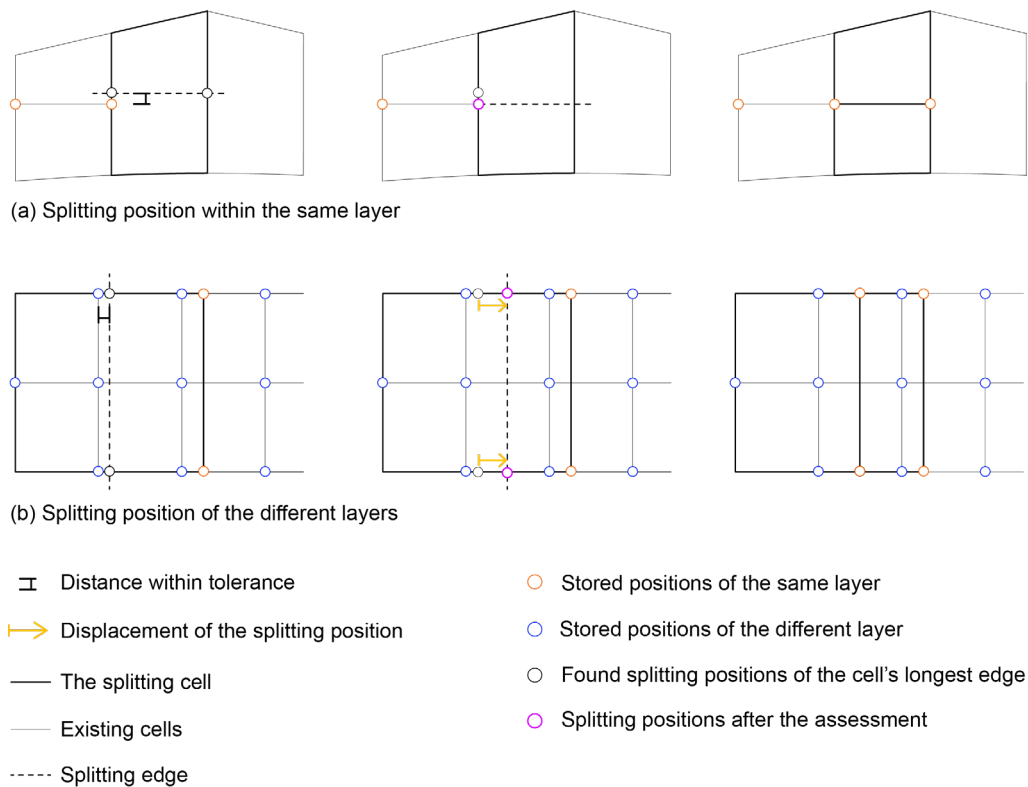


Figure 21: The assessments of splitting points.

The novel method involves preserving the split positions of cells and avoiding the same on the following layer: Each splitting point, along with the corresponding layer index, is stored within a point cloud from RhinoCommon as a class attribute of the cell. The inherited method can find the position of the splitting point faster. Before initiating the splitting procedure, a comprehensive assessment will occur to ascertain each split position's feasibility.

1Suppose a coordinate has been utilized within the same layer or is close to a previously employed position (Fig. 21(a)). In that case, the cell subdivision retains the same splitting position for defining the cutting bounding box. In contrast, when a cell from a different layer divides at or near this place, a deliberate displacement of the splitting position will occur by a random distance, with a more allowable range along the horizontal axis due to the characteristic elongation of beam structures (Fig. 21(b)). This refined position is then employed to define the cutting bounding box for the splitting process precisely. The updated splitting position and its corresponding layer index are saved into the same point cloud, and this procedure will repeat for each iteration of the subdivision of cells. Figure 22 depicts a segmentation result with double LVL boards for a rectangular beam.

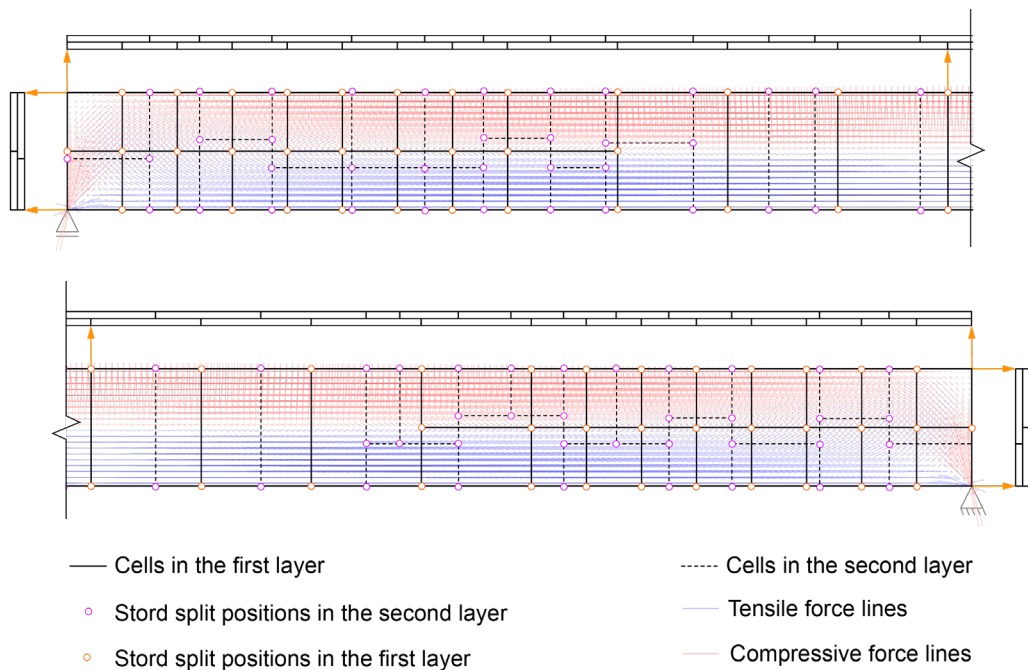


Figure 22: Two layers of segmentation result in parallel projections of their seams compared to the input data for a rectangular beam.

### 3.3.4. Structural Refinery after Segmentations

In further developing this project, integrating a structural analysis from *SOFiSTiK* software can provide valuable refinery into the segmentation results. This software can generate data sets invaluable to engineers for additional evaluation. To streamline this process, users can export the splitting positions with their coordinates directly from the tool into a *.txt* file. This file can then be returned to the engineer for subsequent analysis in *SOFiSTiK*. The exchange of critical structure information ensures that the engineering team is equipped with the most accurate and timely data for decision-making before manufacturing.

The following Figure 23 pictures several outcomes provided by the tool:

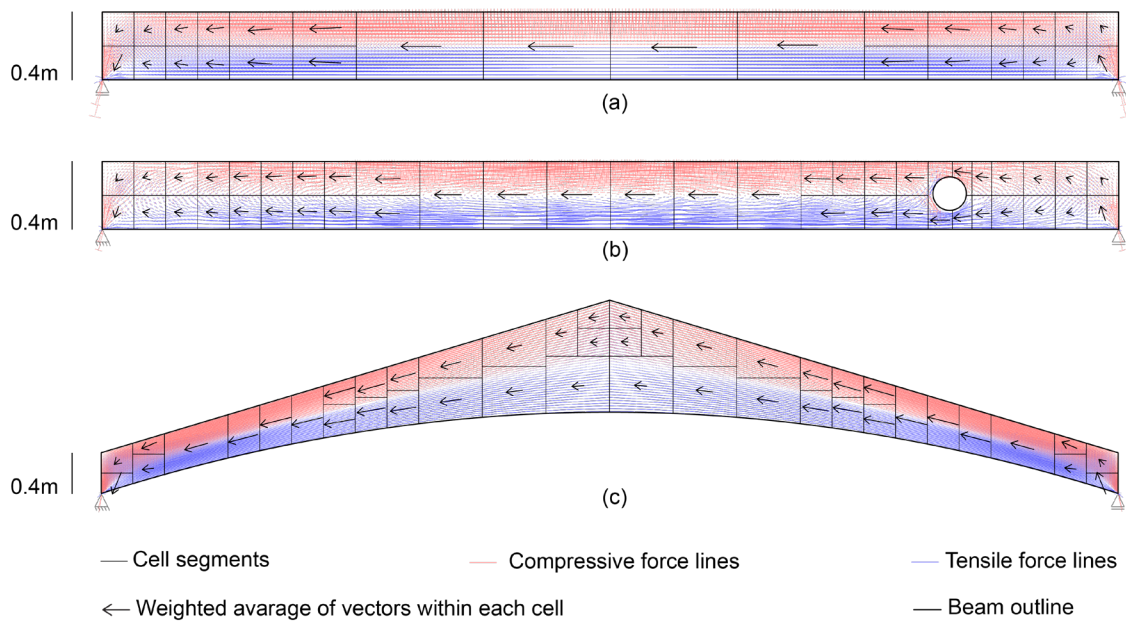


Figure 23: Segmentation results of (a) a rectangular beam, (b) a rectangular beam with a circular cutout, and (c) a pitched cambered beam.

### 3.4. Joints Generation

The tool adds qualifications for producing finger joints and scarf joints for milling paths. Utilizing CNC technology, our industrial partner has the precision and versatility to manufacture various joints, including finger joints, scarf joints, and curved box joints. Moreover, the factory also integrates an additional cutter, particularly for timber finger joint manufacturing. The design tool of this thesis allows attaching joints directly to the milling geometry, which is adjustable for further production methods in the industry.

#### 3.4.1. Neighbouring Finding

The approach of joint generation builds upon the previous cellular segmentation model in the representation of Brep. The objective currently is to create timber joints between these cells. The process involves identifying neighboring for each cell and recording the indices of their contacting faces and edges. An inherited function of Boolean intersection calculates the relationships between segments to identify the contacting faces of the cells (Fig. 24). Using the centroid of this face expedites and simplifies the Boolean calculation. By performing intersections with faces of other segments, neighboring cells, along with their touching face indices and collinear edge indices, are stored for joint generation.

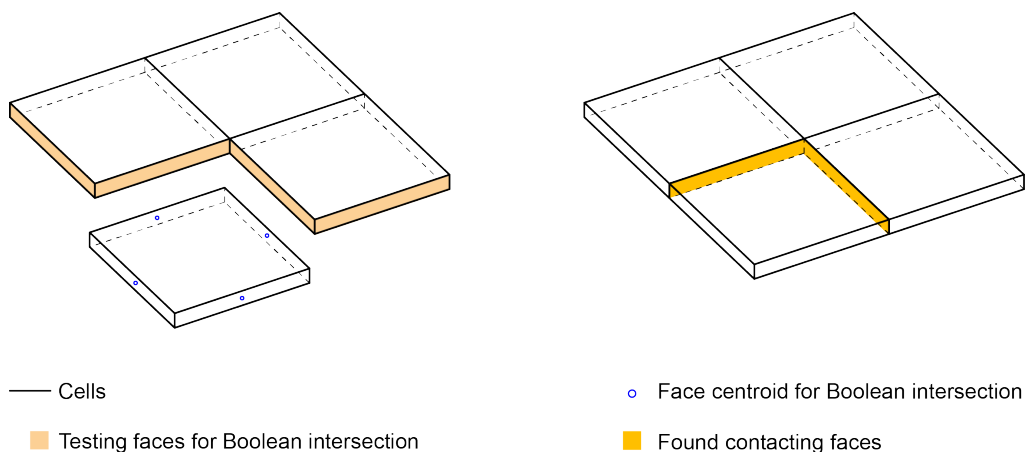


Figure 24: Boolean calculation defining the neighborhood.

### 3.4.2. Finger Joint Generation

The program reworks the stored touching edges to implement finger joints in rectangular patterns. Due to the circular cross-section of CNC milling bits, cutting sharp corners with a CNC is impossible tenon (Fig. 25). For timber joints, it is typically problematic to fabricate a mortise matching a rectangular tenon (Rogeanu et al., 2021).

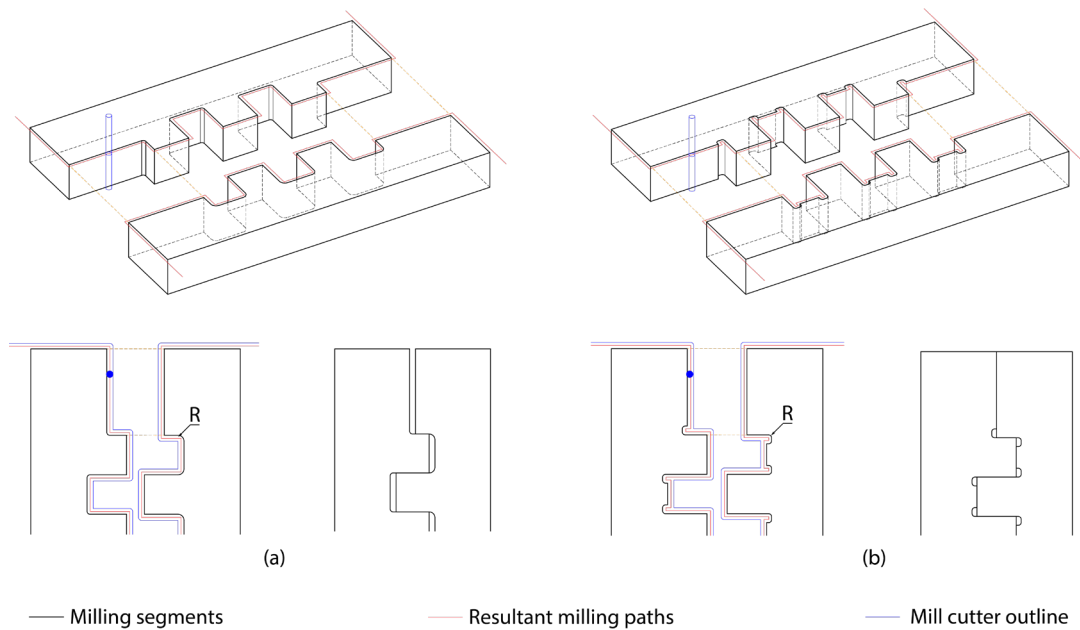


Figure 25: Milling paths for finger joints (a) and with notches (b).

The dimensions of these notches, in terms of width and height, can be specified by users within the design tool (Fig. 26). Another input parameter is the number of joints left out on the end of edges to avoid collisions at the contacting corner. If two contacting edges differ in length, the tool will use a shorter one.

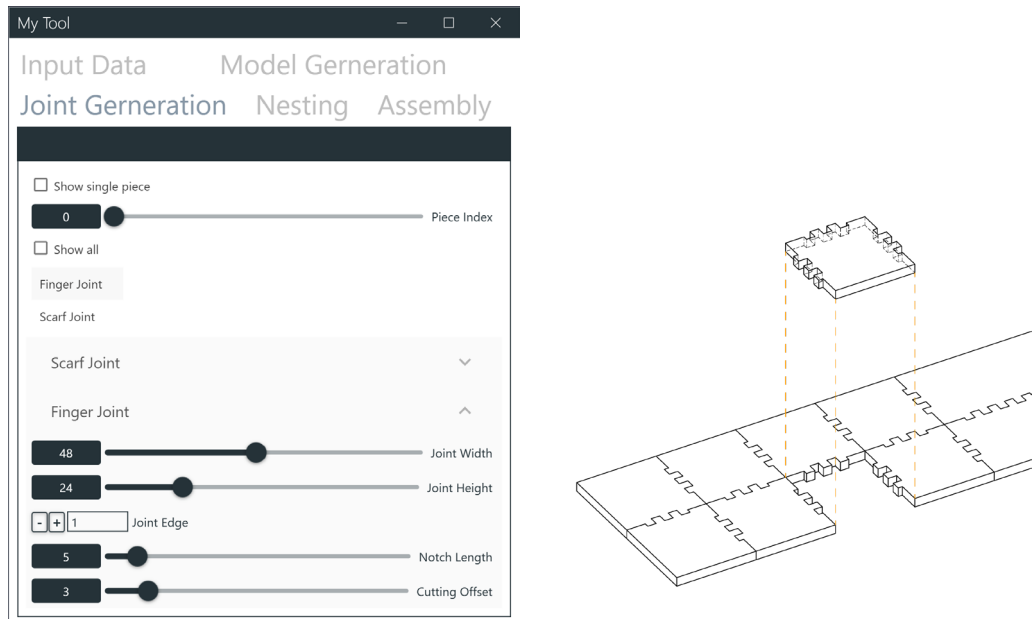


Figure 26: Finger joint generation.

The inherited function of *PointAtLength()* from *RhinoCommon* helps generate control points. The control points are then listed to construct polylines, which are subsequently merged with other edges. The resultant geometry is a closed polyline for milling and an extruded Brep to display the configuration. The following calculation gives the input distance of the function:

$$Distance = Index\ of\ Joint \times Joint\ Width + Edge\ Distance$$

### 3.4.3. Scarf Joint Generation

The thesis also implicates another type of timber joint - plain scarf joint in the design tool. To establish this joint type, the program deforms the contact faces of the segments. Accordingly, vertices are adjusted to a distance counted from the thickness of the plate and the desired cutting angle (Fig. 27). The calculation for shifting distance is:

$$Distance = Thickness \times \tan(Angle)$$

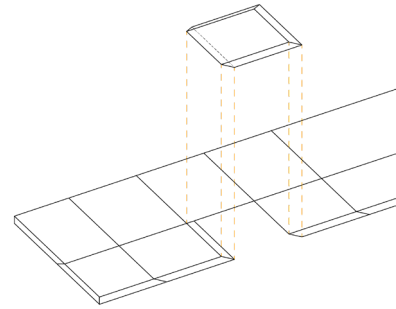
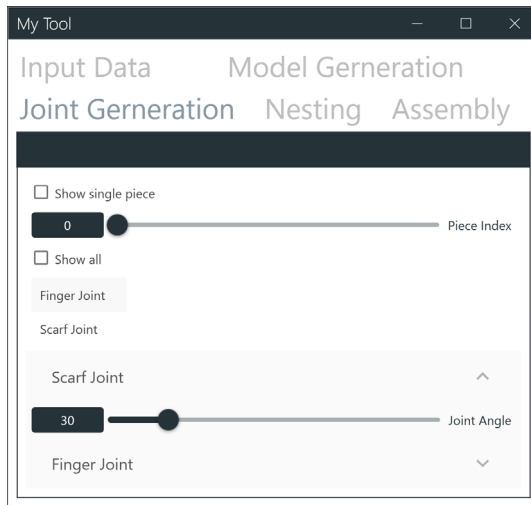
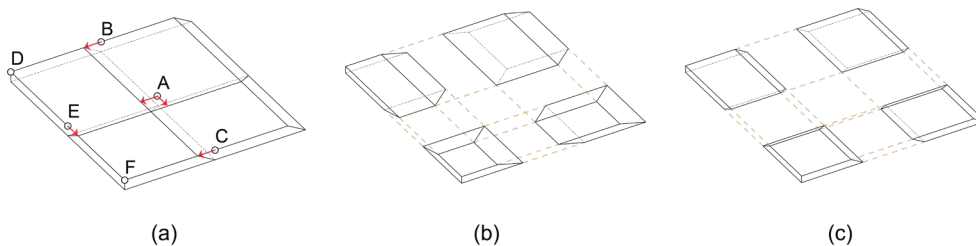


Figure 27: Plain scarf joint generation.

Vertices located on the upper surface of the structure will undergo displacement. The Boolean function evaluates the relationship between vertices' positions and the input structure's boundary before displacing the vertices. If a vertex is on a single boundary surface, it will be shifted at the calculated distance in the horizontal and vertical directions (Point A in Figure 28(a)). Suppose the vertex's location is shared with two faces of the boundary, denoting its placement upon the structure's edge. In that case, the vertex displacement shall proceed along said edge (Point B, Point C, and Point E in Figure 28 (a)). When a vertex is shared by three faces, indicating a structural corner, it will remain at the same position without any displacement (Point D and Point F in Figure 28 (a)). In this way, the global form of the structure remains unchanged after the process. The resultant geometry is a closed Brep volume for milling.



← Shifting distance    ○ Vertices of cell before displacement

Figure 28: Vertex displacement for scarf joint (a), 15° cutting surface in (b), 30° cutting surface in (c).



### 3.5. Nesting and Final Milling Paths

The veneer orientation of individual segments is determined by previously calculating the weighted average of internal forces acting within their region. This orientation is relevant for the fiber direction of the final products. Since the pre-laminated veneer boards settle the fiber grains' direction for milling, the cells rotate based on their orientation vector, aligning them with the global direction of the veneer gains. The global direction can be either horizontal or vertical. The alignment decision is contingent upon the orientation of the milling boards involved.

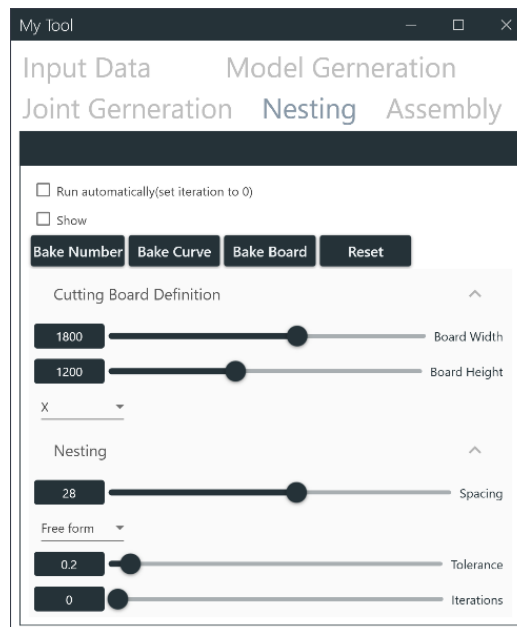


Figure 29: The user interface tab for nesting.

A *Grasshopper* add-on named *OpenNest* further nests the cells' polylines on the desired boards. This plug-in ensures that the cells lay close to each other while limiting their freedom of rotation. The board dimensions, the offset distance among the cells, and the nesting manner are crucial in achieving an optimized nesting arrangement. These are the parameters in the user interface (Fig. 29). It is feasible for users to automate the nesting process. Given visual access to the nesting process, users can utilize veneer boards sufficiently, considering each project's reusability.

An essential criterion for selecting the most suitable arrangement is the usable area enclosed by a rectangle, a universal board shape for reusing, and warehouse storage. Although triangular nesting yields better results, according to *OpenNest*, the practicality of the remaining area must be considered. In comparison among multiple nesting results (Fig. 30), rectangular nesting along a vertical axis left a more practical reusing area. Balancing these considerations enables the identification of the most effective arrangement for the given context. After users decide their nesting result for the final milling, direct outputs of closed polylines, board positions, and numberings of the segments can be done into Rhinoceros via a single mouse click on each corresponding "Bake" button.

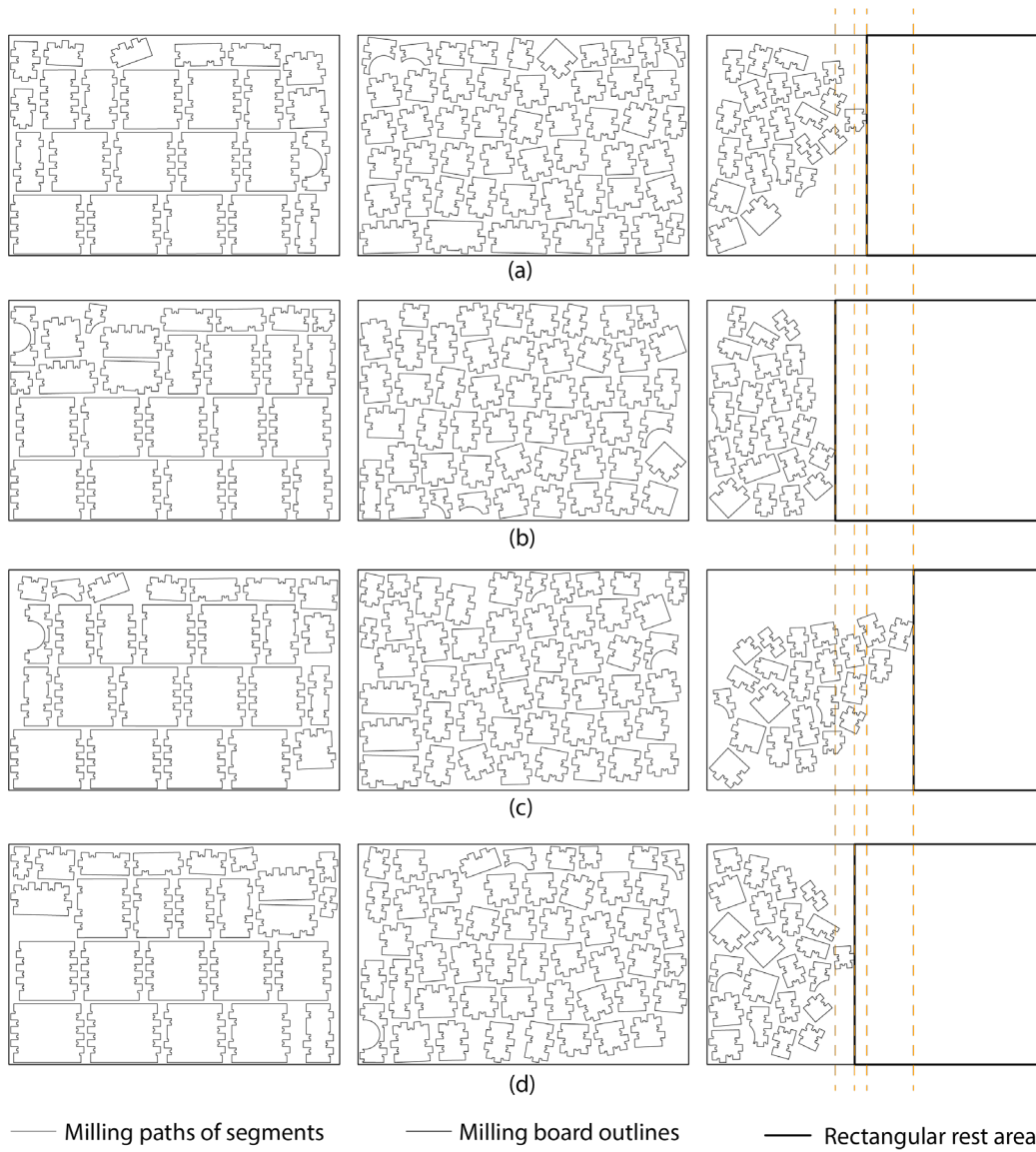


Figure 30: Nesting results with the same segment inputs for an identical board size: OpenNest automates in order from (a) to (d). The rest is marked to compare. (b) gives the largest reusable rectangle.

### 3.6. Interface Design and Assembly Display

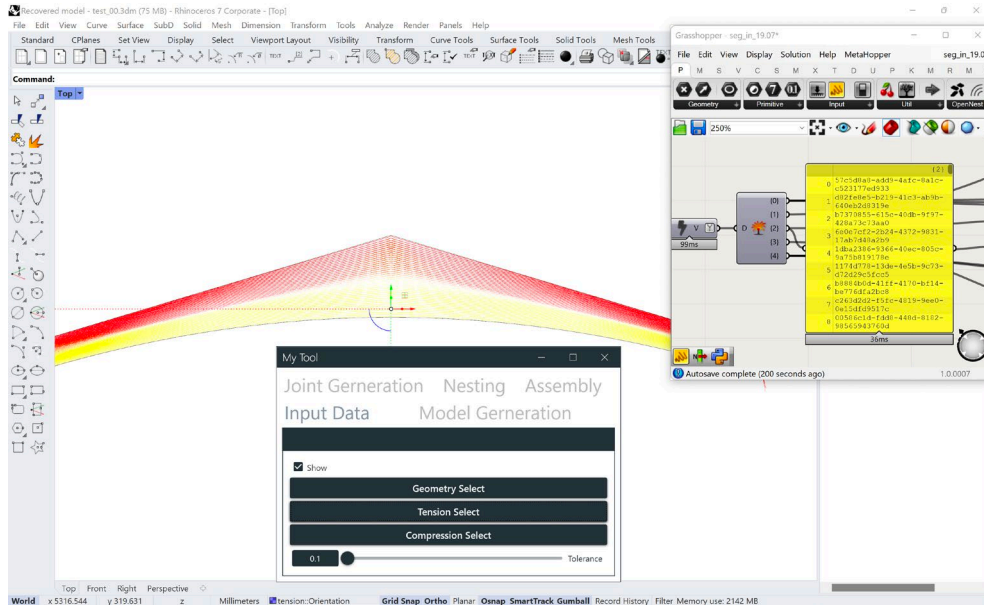


Figure 31: Choosing input lines with the user interface: the data are referenced as *GUID* in *Grasshopper* (right above).

To enhance the tool's usability, the author developed a unified user interface for consolidating multiple *Grasshopper* components with the help of the *UI Plus* plugin. It is an add-on on *Grasshopper* tailored for crafting customized controls within the platform. All pertinent inputs can be set in this tool, streamlining the user experience. In the data feed-in process, users can select all the lines representing forces and a geometrical boundary under the "Input Data" tab in the user interface (Fig. 31). After the selection, components in *Grasshopper* can receive the objects from *Rhinoceros* as their *GUIDs* (short for globally unique identifier) and conduct further calculations in the *Grasshopper*. This effort aligns seamlessly with the overarching design philosophy, which embraces a bottom-up progression strategy. Initiated by the generation of rudimentary geometries, the process gradually advances towards intricate forms, unfolding its complexity. A granular stepwise presentation is facilitated, effectively delineating the developmental journey using segmented tabs and logically grouped inputs. Instead of setting geometries in *Grasshopper's* components, design tool users can import their inputs directly from the

*Rhinoceros* through the interface. Dimensional control is imparted through interactive sliders, and Boolean values are manipulated via dedicated buttons (Fig. 32).

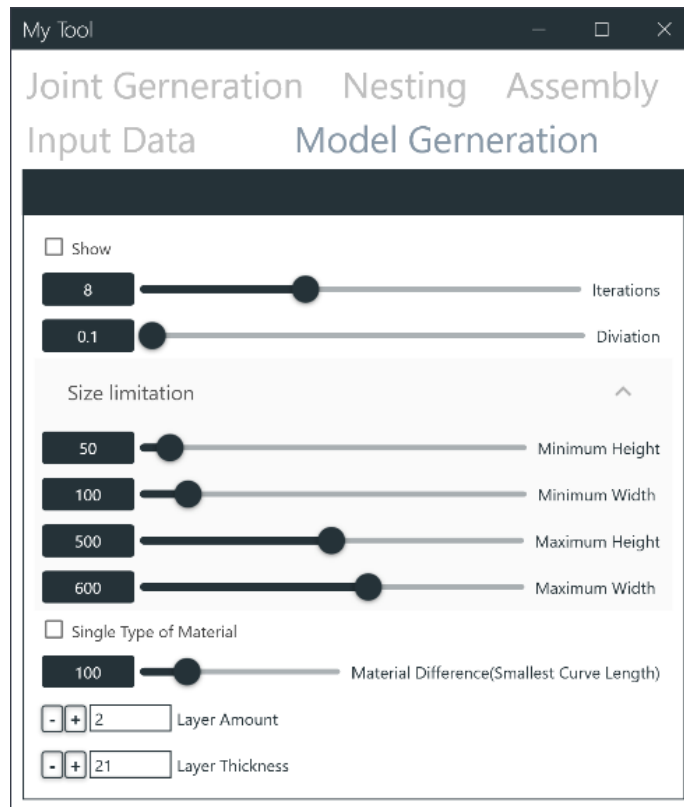


Figure 32: Tabs for modeling with input slides.

For the assembly phase, the user interface provides additional graphical instructions for the sequential presentation of the milled components. The specialized positioning display aids in aligning segments with the overarching structure (Fig. 33).

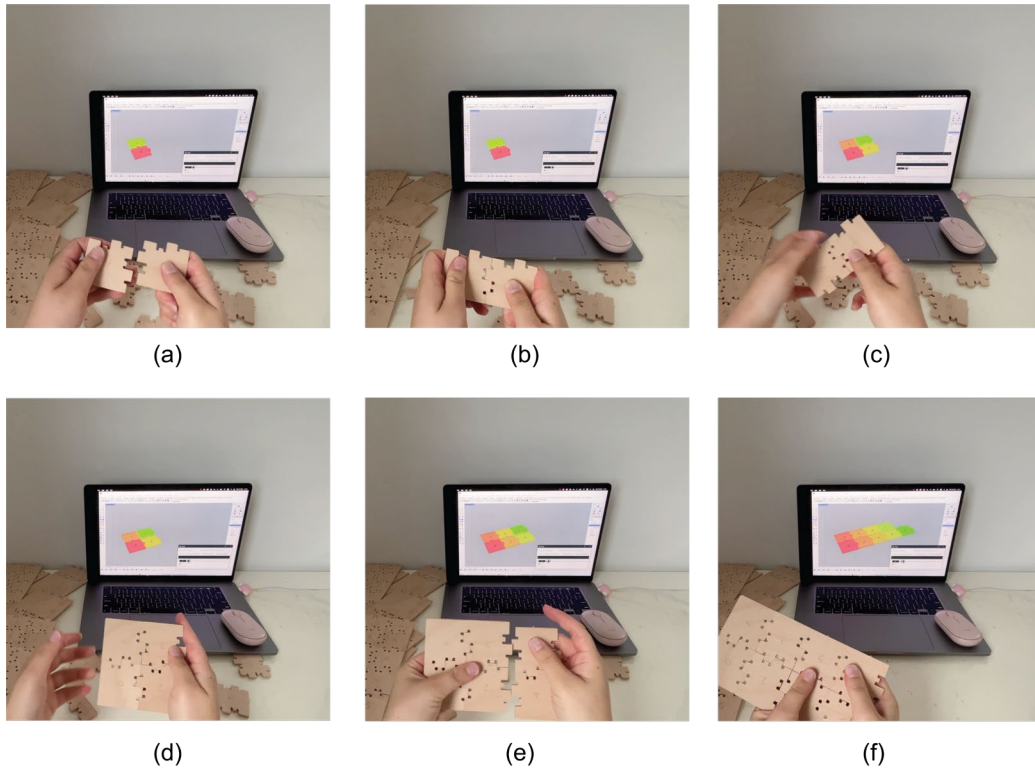


Figure 33: Assembly sequence displays in the user interface.

Due to their rectangular geometry, timber finger joints need to be adeptly inserted in a singular direction. This approach mitigates potential damage from assembling two timber pieces perpendicular to their primary surfaces, which could damage the exposed edge of the veneer fiber. Moreover, a corner piece assembled with inadequate tightness could impede the fitting of subsequent corner segments. A pragmatic approach is embraced to optimize assembly efficiency and circumvent these potential issues: the program groups segments along the shorter direction in the structure, and each step permits solely one side of the component to be assembled.

## 4. Use Case Study – Segmented Timber Beams

### 4.1. Use Cases

In order to validate the functionalities of the design tool, two models are fabricated with separate data from structural analysis:

- A rectangular beam measuring 6m in width and 0.4m in height, with a circular cutout of 0.2m in diameter
- A Pitched cambered beam spanning 10m in width and 0.4m in height, tapering to 1.1m

Table 1 summarizes the essential inputs for the two prototypes. These values relate to the mill cutter's diameter and the machine's milling precision under the condition that the model is scaled to 1:5.

Table 1: Comparison of input data of two prototypes

<b>Structure type</b>	<b>Rectangular beam with a circular cutout</b>	<b>Pitched cambered beam</b>
Dimension of width and height	6m * 0.4m, circular cutout: 0.2m	10m * 0.4 m – 1.1m
Number of compressive forces from the input	13783	75359
Number of tensile forces from the input	3550	31772
Number of layers	2	2
Iteration	8	8
Vectors' deviation for summarizing	0.1	0.3
Maximal width and height of cells	0.6m * 0.5m	0.8m * 0.6m
Minimal width and height of cells	0.05m * 0.1m	0.3m * 0.2m

Structure type	Rectangular beam with a circular cutout	Pitched cambered beam
Minimal output result	50	20
Finger joints' width and height	45 mm * 20 mm	60mm * 30mm
Notches' width and height	10mm * 15mm	13mm * 17.5mm

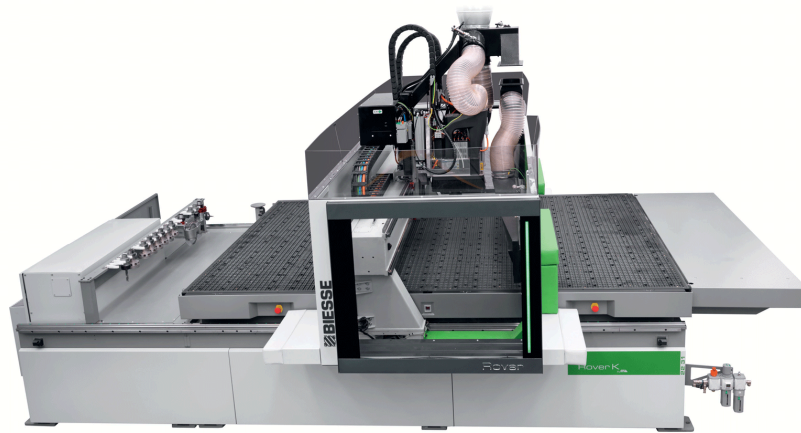


Figure 34: *ROVER CNC milling machine*: Tool change magazine has multiple holders (left) and is available for changing, *BIESSE GROUP 2023*.

In further 1:1 manufacturing in the industry, the producer will choose a thicker mill cutter for a thicker veneer board. For the milling machine *Biesse Rover* with a flexible tooling model (Fig. 34), the industrial manufacturers can choose their milling head's cutter depending on the demanding accuracy and velocity. A mill cutter diameter can vary from 1 cm to 3 cm for a 2.5 cm thick veneer board. The thinner head will take longer since the milling depth should be set similarly to its dimension. Nevertheless, as Chapter 3.4 Joint Generation describes, the final milling path is adjustable with customized inputs.



Segmentation results with finger joints and notches are shown as closed polylines in Figure 35:

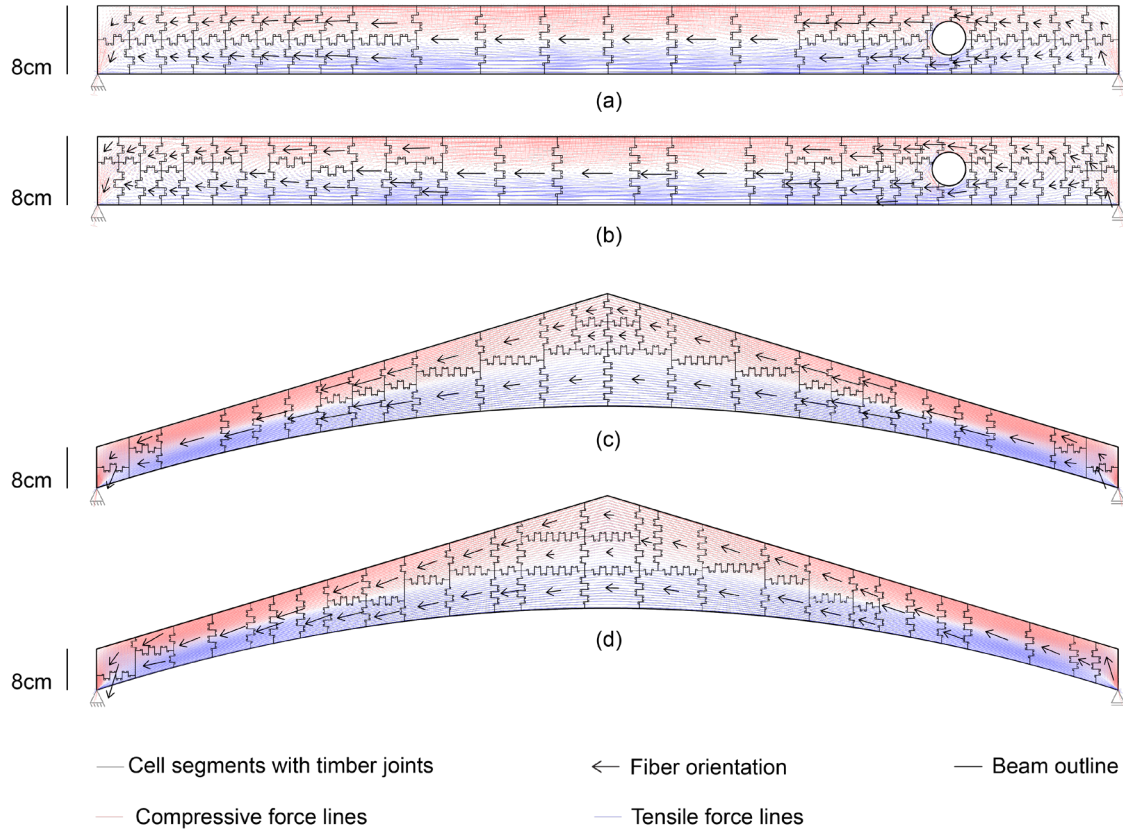


Figure 35: The rectangular beam with a circular cutout, the first LVL layer(a) and the second(b). The pitched cambered beam, the first LVL layer(c) and the second(d). Both are compared their input data.

Table 2 shows almost the same amount of compression vectors in the data filtering process, although the inputs differ in Table 1. Because the end marks of compression values are imported into the feed-in file simultaneously, the number of compressive force lines is much more than the tensile one. After the data filtering, they get nearly even on the amount on both models, which shows the tool's validation despite the inputs' quantities and sizes.

Table 2: Comparison of two segmentation result

<b>Input type</b>	<b>A rectangular beam with a circular cutout</b>	<b>Pitched cambered beam</b>
Number of validated vectors representing compressive forces	2753	18602
Number of validated vectors representing tensile forces	2883	19594
Total number of segments	97	87
Number of segments on first layer	44	44
Number of segments on second layer	53	43
Maximal width and height of segments	458 mm in 69 <sup>th</sup> piece 400 mm (the height of the beam)	655 mm in 4 <sup>th</sup> piece 553 mm in 24 <sup>th</sup> piece
Minimal width and height of segment	84 mm in 94 <sup>th</sup> piece 149 mm in 45 <sup>th</sup> piece	152 mm in 61 <sup>st</sup> piece 143 mm in 86 <sup>th</sup> piece

Both structures are composed of two layers and underwent eight subdivision iterations, with the maximal vectors' deviation set at 0.1 for the rectangular beam and 0.3 for the gabled beam. Their deviation tolerance is derived for two beams according to their dimensions and the input quantities. More extensive input needs a more considerable tolerance. The resultant cells have varying dimensions, all within their desired limitations. As the subdivision results, the rectangular beam comprises 97 segments distributed across two layers. The segment with maximal dimension is in the middle of the structure, where the force distribution changes more smoothly, while the smallest 94<sup>th</sup> and 45<sup>th</sup> pieces are on the structure's edge. The input file shows that internal forces near the supports of the beam differ more than in other areas. The subdivision results of the gabled beam can likewise support the tool's outcome. Because of the dimension constraints, five cells have not reached the targeted average

force deviation, but all the cells' sizes are determined correctly during the subdivision according to the customized settings.

## 4.2. Setup on Digital Cutter

The physical models are fabricated using a professional cutting machine following predetermined milling paths. The machine, operated at the Technical University of Munich, is a Zünd G3 XL-1600 flatbed digital cutter, boasting a processing area measuring 2000 x 1600 mm. The milling head operates along the periphery of the flatbed, as depicted in Figure 36.



Figure 36: The Zünd G3 XL-1600 flatbed digital cutter, Zünd Systemtechnik AG.

Due to the absence of real-time communication capabilities between the design environment in *Rhinoceros* and the machine's control software, planned milling paths necessitate exportation to a .ai file prior to transmission to the controller. The *Zünd Cut Center* software facilitates this translation process, which

integrates through a plugin on *Adobe Illustrator*. After exporting the milling path as *Illustrator's* data from the *Rhinoceros* environment, the *Zund Cut Center* translates the geometries in closed polylines into the requisite machine code for the cutter. The software also can detect disconnected or minute milling paths and potential collisions between geometries.

The selection of the mill cutter for the milling head is contingent upon the processed material's thickness. This experiment utilizes a 3mm milling head for 4mm thick laminated veneer plates. As the cutter's milling depth approximates its diameter, it repeats twice to traverse the 4mm veneer plates completely. The *Zund Cut Center* software automates this process based on customized material thickness and cutting head dimensions. Moreover, manufacturers can willingly adjust milling velocity and cutting depth. Notably, dimensions for notches on concave corners are set following the milling head's dimensions. These notches possess a depth of 2mm, slightly exceeding the 1.5mm radius of the mill cutter, and a width of 3mm (scaled from 10mm \* 15mm in a 1:5 ratio).

### 4.3. Veneer Milling Process

To gather wasted woodchips during milling, an additional vacuum pipe is affixed to the milling head module, as shown in Figure 37. The vacuum table holds the LVL boards in place. Additionally, several timber connectors are attached to the geometry (Fig. 37) on the *Zund Cut Center* platform to stabilize the cut pieces after milling. These delicate connectors, called bridges, remain uncut on the final layer on milling paths. They have an average thickness of approximately 1mm.

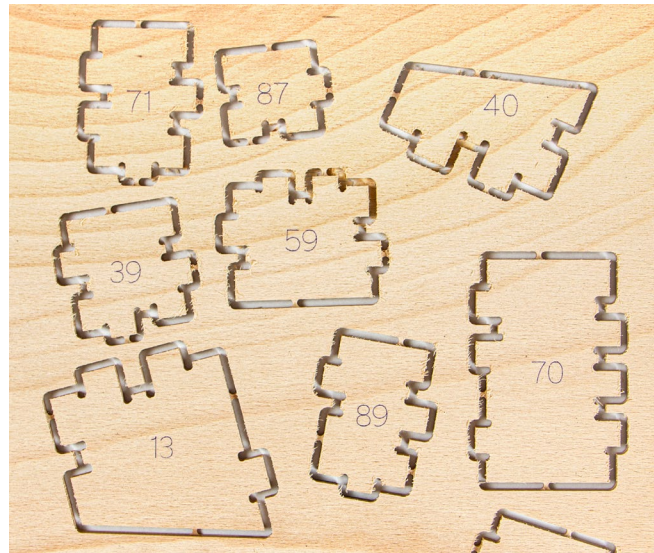


Figure 37: Bridges connect the cut pieces and the board.

Due to the floating of air on surface, some of these bridges may break during milling. This issue happened particularly at the edges of the veneer plates, where the plates experience bending due to humidity. The bridges are more vulnerable here, as the initial cutting round goes deeper than intended. In such cases, the digital cutter must be manually paused. The supervisor should carefully extract the detached piece by hand to prevent it from flipping out and potentially being destroyed by the mill cutter. The digital cutter's drawing module facilitates piece numbering (Fig. 38). Unlike a laser cutter producing melting marks, a simple ballpen-end module conserves energy and yields cleaner numbering results.

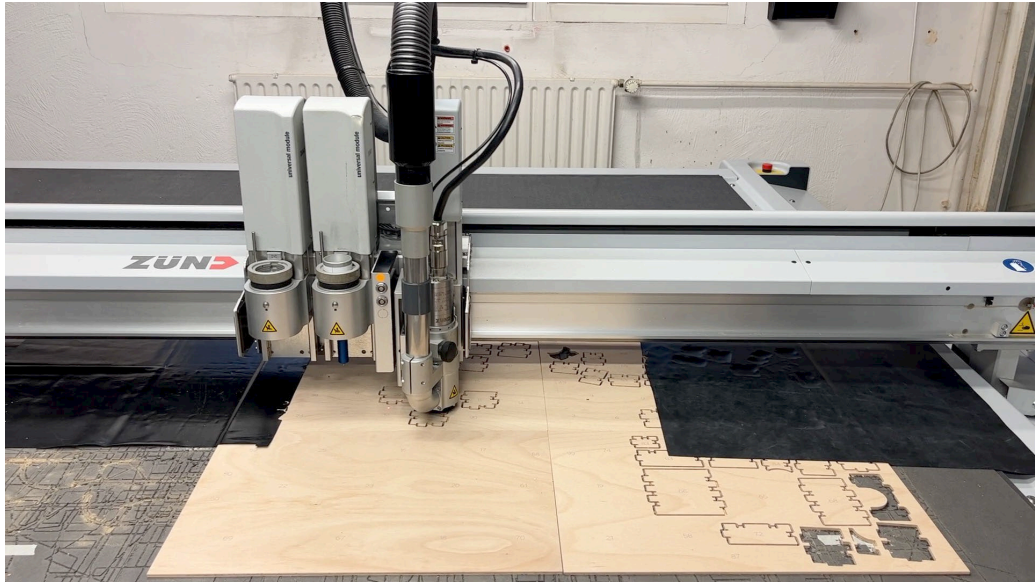


Figure 38: The Zünd G3 flatbed digital cutter with two assembled model: the mill cutter (right) and the drawing module with a ball-pen end (middle in blue).

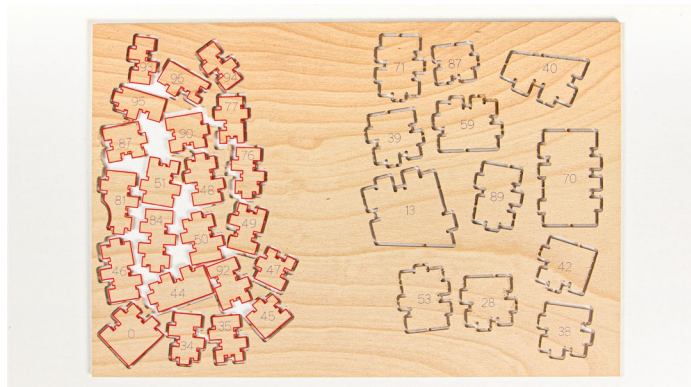


Figure 39: The nesting result generated in the design tool (left outlines in red) and the pieces on the second round (right).

Upon the first round of milling, any failed pieces are documented. The *Integrated Compact Color* camera module, present in the digital cutter, assists in identifying the remaining space on the used boards. This information enables the arrangement of new milling paths within the unused material. Consequently, the second round of milling takes place on the existing board (Fig. 39). This process exemplifies the significance of the nesting process in the design tool, as it saves veneer materials and promotes sustainability in the industry.



## 5. Results

To validate the feasibility of the developed structure, I apply the design tool described in Chapter 3 to compute two given beam structures. The demonstrator objects are fabricated through a digital cutter from the Design Factory at the Technical University of Munich. Chapter 4 describes the utilization of the design tool, related milling path solutions, milling machines, and materials. The following chapter is structured in an illustration of the outcomes of the thesis, followed by a description of the result of the demonstrator milling.

### 5.1. Summary

The thesis results summarize on different scales, both in theory and practice, which are described as follows.

Foremost, a segmentation strategy followed by the forces distribution of a customized structure was delineated, illustrating how the segmentation behavior of systems can be guided by internal force flow orientation. Integrating a cellular division inspired algorithm, the thesis developed a unique segmentation and modeling strategy for capturing the subdivision behavior overfitting the force flow orientation within a predefined boundary, which was pivotal in fabricating the desired beam structure.

Secondly, the internal force distribution drove the orientation of veneer grains on segments. This novel arrangement of veneer fiber to build up the reinforcement of veneer-reinforced timber structure expands the utilization of laminated veneer lumber. I constructed the strategy on an analytical design-to-fabrication approach, which streamlined the translation of reliable structural analysis data into design input parameters.

In addition, the thesis led to the development of a compact design tool that bridges structural analysis and fabrication outcomes, marking an innovation in the generation tool of milling paths. The author explored an intriguing alternative concerning the arrangement of veneers. Rather than a conventional parallel direction bond, this approach capitalizes on the reaction to force distributions, potentially expanding veneer manufacturing methods.

The thesis also introduced enhanced user control over the veneer milling paths by the design tool, extending beyond mere beam structure segmentation. This improved control encapsulates joint generation and the nesting of geometries on final boards, promising better material utilization and sustainability. Notably, this nesting process demonstrated potential for material conservation while ensuring improved structural behavior with consistent material resources.

Hands-on experiences from the milling process enriched the study, offering insights into the practicalities of using milling machines. The tool's design was meticulously carried out in the awareness of the CNC milling fabrication method. At the end of the study, the author successfully built up segmented prototype models with a milling machine at a 1:5 scale, detailed in the next chapter. These will soon be translated into a final 1:1 mock-up with the help of the industrial partner, setting the stage for a final presentation and subsequent verification.



## 5.2. Fabrication of Prototypes

As described in the last section, two beam structures are segmented, and the design tool generates their milling paths. Both models are fabricated on the scale of 1:5 with 4mm thick standard laminated veneer plates.

The 6m \* 0.4m rectangular beam incorporating a circular cutout is divided into 97 pieces, arranged on three veneer boards with dimensions of 460mm by 310mm (Fig. 40, (a) to (c)). On a scale of 1:5, this beam has a total milling path length of 24,908mm. The residual functional area left on these boards amounts to 83,820mm<sup>2</sup>, around 20% of the total area of the last veneer board (Fig. 40 (c)). I arranged the failed pieces on this left material on the second milling round (Fig. 40, (c)). The machine takes approximately 70 minutes for this model, exclusive of any setup or adjustment time. There are three bridges on each piece. However, its production has a higher margin of error, with a reported ten pieces turning out as failures.

The second 10m \* 0.7m model is a pitched cambered beam. Its milling path is notably longer for the 87 pieces, measuring 41,479mm on the 1:5 scale (Fig. 40, (d) to (g)). The production of this beam uses four timber boards, each measuring 610mm by 410mm. 15% of the last boards offer a proper residual area of 142,186 mm<sup>2</sup> (Fig. 40 (g)). Milling this more intricate design requires more time, with the process taking approximately 120 minutes without considering machine adjustments. Nevertheless, despite its complexity, this beam exhibits a lower failure rate with two bridges on each piece, with only two pieces reported as defective.

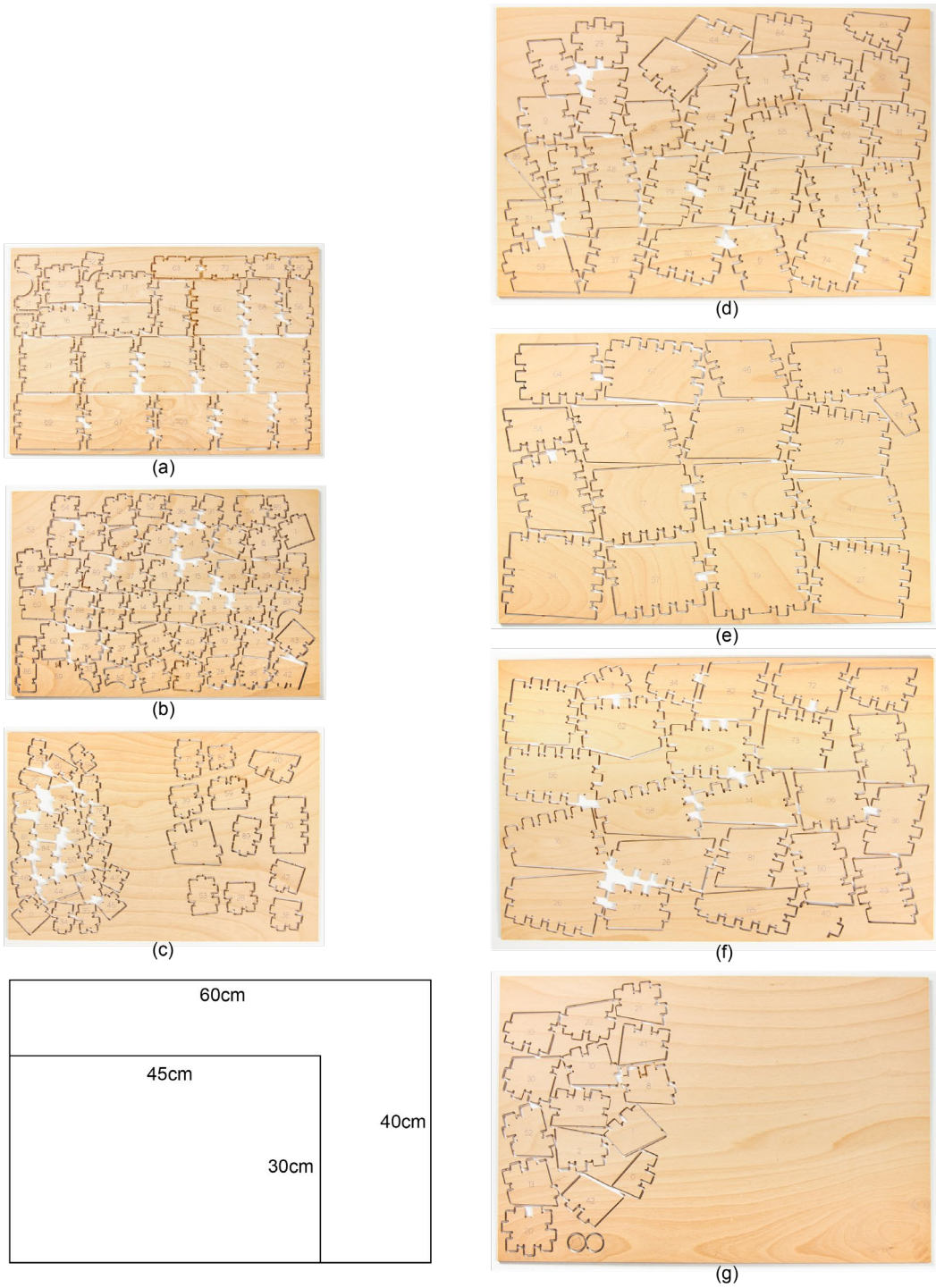


Figure 40: Milling results of the rectangular beam from (a) to (c), and the pitched cambered beam from (d) to (g).

### 5.3. Milling with the Digital Cutter

The digital cutter's high accuracy level ensures that the veneer orientations are executed precisely as planned. After assembly, Figure 41 and Figure 42 illustrate the two segmented models, showcasing their detailed components. The high similarity between the generated milling paths and their orientations with the built models indicates a promising outcome from the design tool and this novel algorithm (Fig. 43 and Fig. 44).

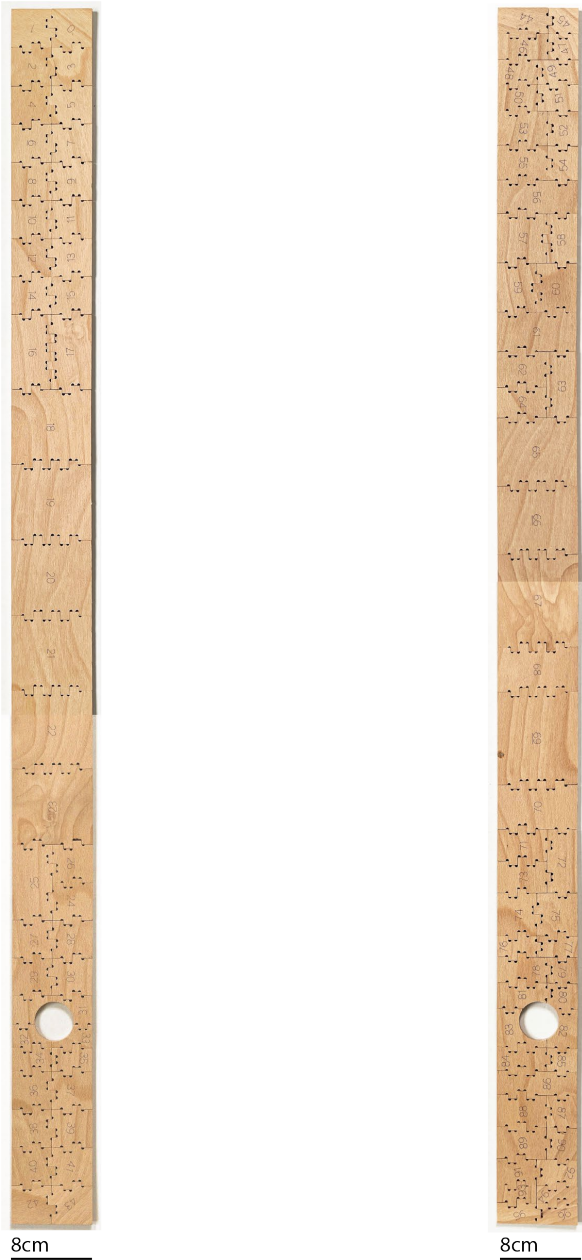
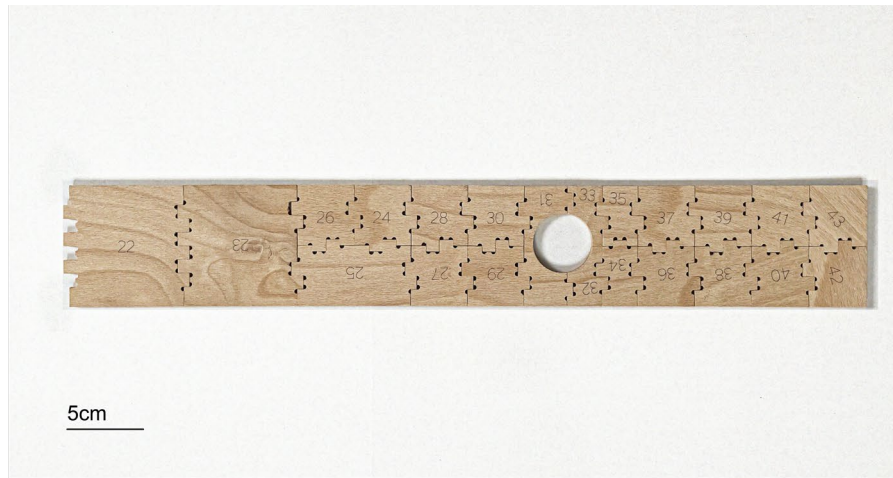


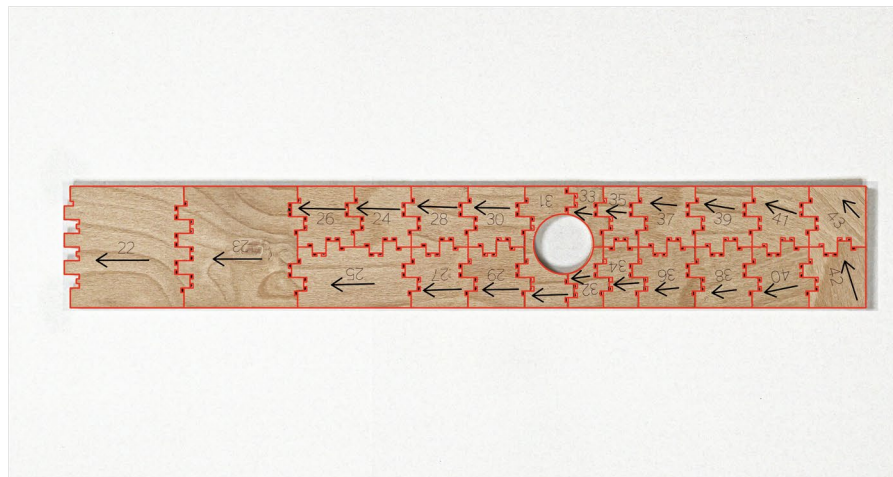
Figure 41: The rectangular beam with a circular cutout, the first segmentation layer on the left, and the second on the right.



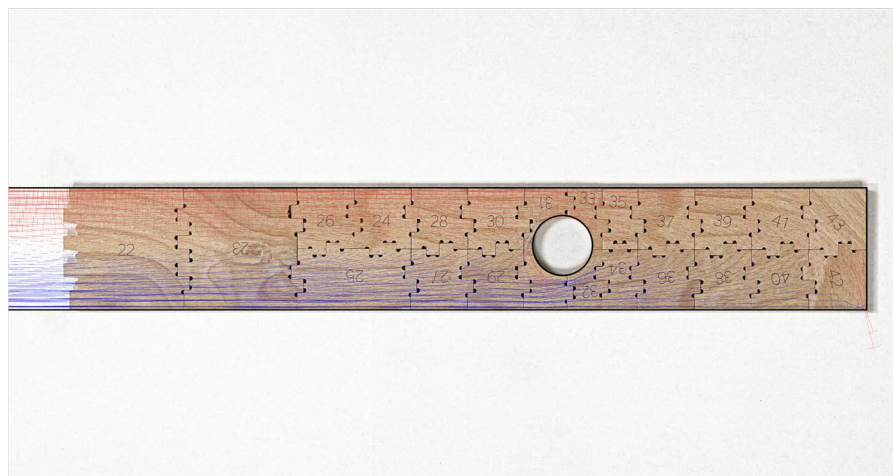
Figure 42: The pitched cambered beam, the first segmentation layer on the left, and the second on the right.



(a)



(b)

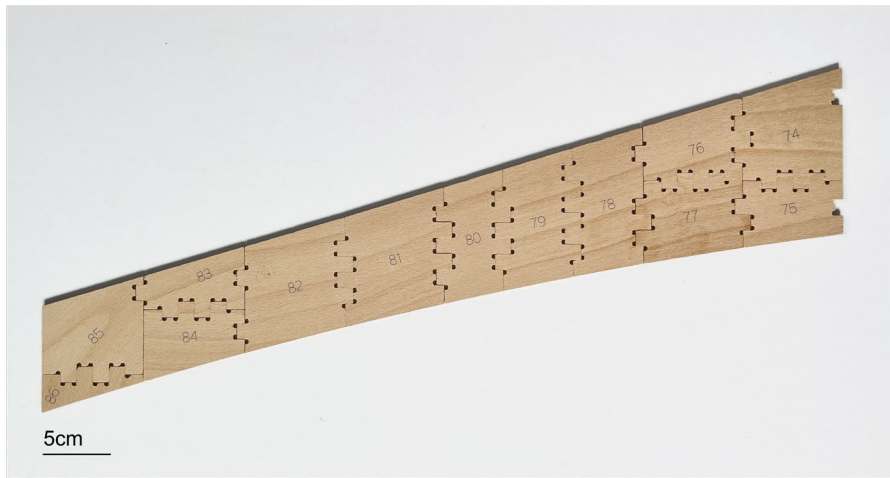


(c)

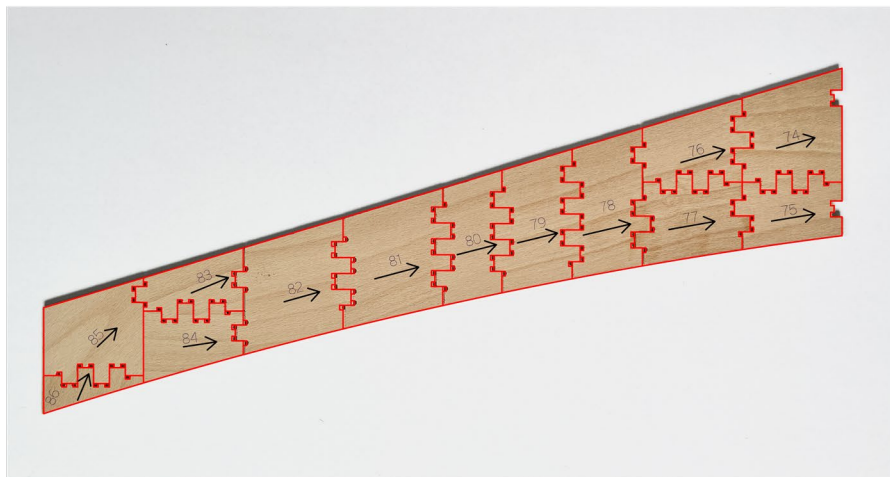
— Resultant milling paths     $\leftarrow$  Resultant veneer orientations    — Beam outline  
— Compressive force lines    — Tensile force lines

Figure 43: Part of the rectangular beam with the circular cutout(a), in comparison with (b) the planned milling paths and (c) the input data of structural analysis.

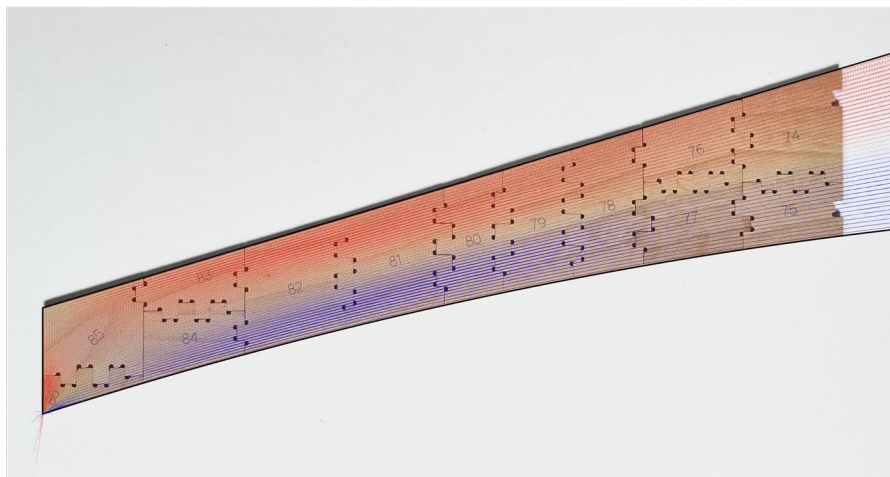




(a)



(b)



(c)

- Resultant milling paths      ← Resultant veneer orientations      — Beam outline
- Compressive force lines      — Tensile force lines

Figure 44: Part of the pitched cambered beam (a), in comparison with (b) the planned milling paths and (c) the input data of structural analysis.

Three reasons have been identified for the milling failures in this prototype experiment:

Firstly, inadequate spacing between pieces affects the vacuum table's ability to hold the board onto the digital cutter securely. This instability can lead to imprecise cuts and, subsequently, defective pieces.

Secondly, placing some bridges in the left-over areas on veneer boards contributes to issues. Specifically, this poor placement causes the detachment of pieces from the board during milling, leading to further failures.

Lastly, deformations observed in the beech LVL boards, particularly on the edges, result in milling inaccuracies. This issue is most evident in the mill depth, which leads to thinner bridges that cannot meet the stiffness requirements to connect the components and the rest of the board (Fig. 45).

Each of these factors poses a unique challenge to the milling process, impacting both the time efficiency and the quality of the finished product. The failed geometries are manually arranged on the remaining veneer boards and remade with an extra bridge on each for the second round.

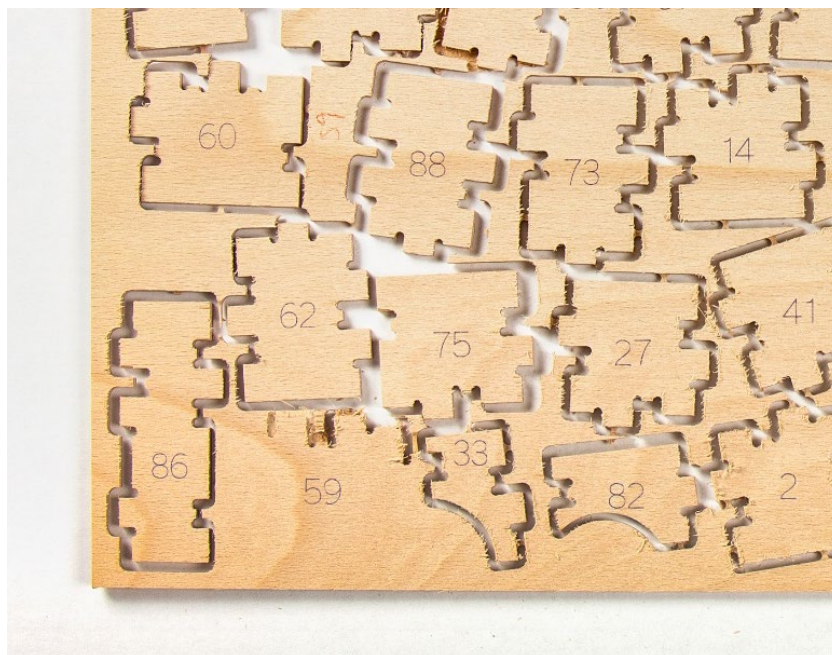


Figure 45: Failed cutting on the board's edge.

## 6. Conclusion

### 6.1. Discussion

The thesis embarks on a multidisciplinary journey intersecting computational modeling and design, structural engineering, and digitally assisted fabrication. The work provides an integrated computational design tool enabling architects and engineers to fabricate custom, high-performance superlamella beams from standard laminated veneer plates.

In terms of conceptual achievements, this thesis proposes a force-flow-oriented segmentation strategy built on imitating cellular division algorithms. The significance of this approach lies in its potential to align veneer layers in a manner responsive to internal force distributions, thereby improving the structural behavior of the resultant timber beam. The computational tool developed successfully captured this complex behavior and facilitated an efficient translation of these insights into actionable fabrication paths.

The design tool application extends beyond the arrangement of veneers; it provides enhanced user control over milling paths, joint generation, and geometries nesting on the material. This dual focus on structure-aware fabrication and resource conservation makes it a comprehensive solution for the modern timber construction industry's challenges.

Hands-on prototyping experiments validated the tool's feasibility. Through these experiments, the study shed light on the practical aspects of digitally assisted fabrication, specifically CNC milling methods, thus bridging the gap between computational design and physical manufacturing.



## 6.2. Future Work

The thesis proves the feasibility of the segmentation and fabrication concept for non-standard superlamella through physical prototypes. Further structural analysis from the engineering team in the Chair of Timber Structures and Building Construction at the Technical University of Munich will serve as a critical validation for the segmented models generated through the computational tool, thus closing the loop between computational design and structural engineering.

Additionally, *OWI GmbH* (Fig. 46) the industrial partner of the Chair of Digital Fabrication at the Technical University of Munich, will provide a 1:1 use-case prototype fabrication, which is scheduled at the end of September 2023, after the submission of this master thesis. Collaborating with the industry can help refine the design tool to cater to specific market demands and ensure its relevance in real-world applications.



Figure 46: Biesse CNC Milling machine, utilizing in OWI GmbH, BIESSE GROUP 2023.

The prototypes fabricated on a scale of 1:4 show that the predicted veneer orientation is in accord with the physical models. Supposedly, it successfully improves the strengths and stiffness of the veneer structure. In this case, the veneer manufacturing industry can further utilize the outcomes of this research in optimizing the fabrication methods of laminated veneer lumber products. The segmentation of customized load-bearing structures for CNC milling could follow the principle developed in this thesis (Fig. 47).



Figure 47: Possible future utilization of this thesis: force-flow oriented segmentations for CNC milling veneer production.

## 7. Bibliography

DIN EN 14279. (2009). *DIN EN 14279, Furnierschichtholz (LVL) – Definitionen, Klassifizierung und Spezifikationen; Deutsche Fassung EN 14279:2004+A1:2009*. Normenausschuss Holzwirtschaft und Möbel (NHM) im DIN, Deutsches Institut für Normung.

DIN EN 14374. (2004). *DIN EN 14374, Holzbauwerke – Furnierschichtholz für tragende Zwecke – Anforderungen; Deutsche Fassung EN 14374:2004*. Normenausschuss Bauwesen (NABau), Deutsches Institut für Normung.

D. Mans, *Ui Plus*. Retrieved August 23, 2023, from <https://www.food4rhino.com/en/app/ui>

Graf, P., Lohmann, B., & Boldt, B. (2022). *Bioeconomy in Germany - Opportunities for a bio-based and sustainable future*. Federal Ministry of Food (BMBF) and Agriculture and Federal Ministry of Food and Agriculture (BMEL). Retrieved August 23, 2023, from [https://www.bmbf.de/pub/Biooekonomie\\_in\\_Deutschland\\_Eng.pdf%5Cn](https://www.bmbf.de/pub/Biooekonomie_in_Deutschland_Eng.pdf%5Cn)

Heitkamp, T., Kuschmitz, S., Girnth, S., Marx, J. D., Klawitter, G., Waldt, N., & Vietor, T. (2022). Stress-adapted fiber orientation along the principal stress directions for continuous fiber-reinforced material extrusion. *Progress in Additive Manufacturing*, 0123456789. <https://doi.org/10.1007/s40964-022-00347-x>

Kagermann, H., Wahlster, W., & Helbig, J. (2013). Umsetzungsempfehlungen für das Zukunftsprojekt Industrie 4.0 - Abschlussbericht des Arbeitskreises Industrie 4.0. *Plattform Industrie 4.0, April*, 1–116. Retrieved August 23, 2023 from [https://www.bmbf.de/pub/Biooekonomie\\_in\\_Deutschland\\_Eng.pdf%5Cn](https://www.bmbf.de/pub/Biooekonomie_in_Deutschland_Eng.pdf%5Cn)

Kizilörenli, E., & Maden, F. (2021). Tessellation in Architecture from Past to Present. *IOP Conference Series: Materials Science and Engineering*, 1203(3), 032062. <https://doi.org/10.1088/1757-899x/1203/3/032062>

Klemmt, C., & Sugihara, S. (2020). Architectural Design by Cellular Growth Algorithm. *ALIFE 2018 - 2018 Conference on Artificial Life: Beyond AI*, 548–549. [https://doi.org/https://doi.org/10.1162/isal\\_a\\_00102](https://doi.org/https://doi.org/10.1162/isal_a_00102)

Lechner, M. (2020). Hybride Holzbauteile aus Laubholz-Furnieren und Brettschichtholz aus Nadelholz – holzbewehrtes Holz. *Conference: 8. Doktorandenkolloquium Holzbau Forschung + Praxis 2020A · At: Stuttgart*. Retrieved August 23, 2023, from <https://www.researchgate.net/publication/339954230>

Lechner, M. (2021). Holzbewehrtes Holz. Retrieved August 23, 2023 from <https://mediatum.ub.tum.de/?id=1614846>

Lechner, M., Dietsch, P., & Winter, S. (2021). VENEER-REINFORCED TIMBER. *WCTE, online*. August. <https://doi.org/10.14459/2021md1621533>

L. Vestarte & P. Vestartas, *OpenNest*. Retrieved August 23, 2023 from <https://www.food4rhino.com/en/app/opennest>

Python Software Foundation, *Welcome to Python.org*. Retrieved August 23, 2023 from <https://www.python.org/>

Robert McNeel & Associates, *RhinoCommon API*. Retrieved August 23, 2023 from <https://developer.rhino3d.com/api/RhinoCommon/>

Rogean, N., Latteur, P., & Weinand, Y. (2021). An integrated design tool for timber plate structures to generate joints geometry, fabrication toolpath, and robot trajectories. *Automation in Construction*, 130(July), 103875. <https://doi.org/10.1016/j.autcon.2021.103875>

Sonntag, D., Aldinger, L., Bechert, S., Alvarez, M., Groenewolt, A., Krieg, O. D., Wagner, H. J., Knippers, J., & Menges, A. (2019). Lightweight segmented timber shell for the Bundesgartenschau 2019 in Heilbronn. *IASS Symposium 2019 - 60th Anniversary Symposium of the International Association for Shell and Spatial Structures; Structural Membranes 2019 - 9th International Conference on Textile Composites and Inflatable Structures, FORM and FORCE, October* 2669–2676.

Tam, K. M. M., & Mueller, C. T. (2017). Additive Manufacturing Along Principal Stress Lines. *3D Printing and Additive Manufacturing*, 4(2), 63–81. <https://doi.org/10.1089/3dp.2017.0001>

Wagner, H. J., Alvarez, M., Groenewolt, A., & Menges, A. (2020). Towards digital automation flexibility in large-scale timber construction: integrative robotic prefabrication and co-design of the BUGA Wood Pavilion. *Construction Robotics*, 4(3–4), 187–204. <https://doi.org/10.1007/s41693-020-00038-5>

Wittchen, B., Josten, E., & Reiche, T. (2006). *Holzfachkunde - Ein Lehr-, Lern- und Arbeitsbuch für Tischler / Schreiner und Holzmechaniker*. Teubner.

Zünd Systemtechnik AG. (2020). *Zünd Cut Center 3.3 (10-2020) - Essential new features* (Vol. 3). Retrieved August 23, 2023, from [www.zund.com](http://www.zund.com)

## 8. List of Figures

Figure 1: The interior renovation project was nested onto 1200 3.6m * 1.2 m plywood sheets and milled using a small 3-axis CNC router, <i>dECOi Architects</i> .9	
Figure 2: Principal structure of veneer-reinforced timber, Markus Lechner.....	10
Figure 3: A possible arrangement of veneer for non-standard superlamella in pitched cambered beam, Markus Lechner. ....	11
Figure 4: Research objectives.....	12
Figure 5: Software platform.....	14
Figure 6: The resulting specimens, Kam-Ming Mark Tam and Caitlin Mueller.	15
Figure 7: Exemplary process flow for generating a stress-adapted infill pattern. ....	16
Figure 8: Interior of the building demonstrator, ICD/ITKE University of Stuttgart. ....	17
Figure 9: Photo of Gaizoshoku in the Lobby, Christoph Klemmt. ....	18
Figure 10: Possible arrangements of veneers in VRT, Markus Lechner. ....	19
Figure 11: Veneer arrangements in VRT, Markus Lechner. ....	20
Figure 12: Production of veneer strips glued parallel to the fibers as a preliminary product to produce veneer-reinforced timber, Lechner Markus. ....	21
Figure 13: Workflow of the design tool. ....	22
Figure 14: Part of the input file of a rectangular beam in <i>Rhinoceros 7.0</i> (left), the same part after data filtering in <i>Grasshopper</i> (right). ....	24
Figure 15: A principal sketch on finding dimension lines on a zoomed-in of input data. ....	25

Figure 16: Vector results in <i>Grasshopper</i> after data filtering.....	25
Figure 17: Concept of the cellular division modeling. ....	26
Figure 18: Cell state definition constraints on one iteration .....	27
Figure 19: Different sizes of "cells" with their weighted average vectors compared to the input data for a pitched cambered beam.....	28
Figure 20: Cell subdivision (a) horizontally and (b)vertically, cells after subdivision (c) compared to the input data for a pitched cambered beam. ....	29
Figure 21: The assessments of splitting points.....	30
Figure 22: Two layers of segmentation result in parallel projections of their seams compared to the input data for a rectangular beam.....	31
Figure 23: Segmentation results of (a) a rectangular beam, (b) a rectangular beam with a circular cutout, and (c) a pitched cambered beam.....	32
Figure 24: Boolean calculation defining the neighborhood. ....	33
Figure 25: Milling paths for finger joints (a) and with notches (b).....	34
Figure 26: Finger joint generation. ....	35
Figure 27: Plain scarf joint generation. ....	36
Figure 28: Vertex displacement for scarf joint (a), 15° cutting surface in (b), 30° cutting surface in (c).....	36
Figure 29: The user interface tab for nesting.....	37
Figure 30: Nesting results with the same segment inputs for an identical board size: OpenNest automates in order from (a) to (d). The rest is marked to compare. (b) gives the largest reusable rectangle.....	39
Figure 31: Choosing input lines with the user interface: the data are referenced as <i>GUID</i> in <i>Grasshopper</i> (right above).....	40

Figure 32: Tabs for modeling with input slides. ....	41
Figure 33: Assembly sequence displays in the user interface. ....	42
Figure 34: <i>ROVER CNC milling machine</i> : Tool change magazine has multiple holders (left) and is available for changing, <i>BIESSE GROUP 2023</i> .....	44
Figure 35: The rectangular beam with a circular cutout, the first LVL layer(a) and the second(b). The pitched cambered beam, the first LVL layer(c) and the second(d). Both are compared their input data. ....	45
Figure 36: The Zünd G3 XL-1600 flatbed digital cutter, <i>Zünd Systemtechnik AG</i> . ....	47
Figure 37: Bridges connect the cut pieces and the board.....	49
Figure 38: The Zünd G3 flatbed digital cutter with two assembled model: the mill cutter (right) and the drawing module with a ball-pen end (middle in blue). ....	50
Figure 39: The nesting result generated in the design tool (left outlines in red) and the pieces on the second round (right). ....	50
Figure 40: Milling results of the rectangular beam from (a) to (c), and the pitched cambered beam from (d) to (g). ....	54
Figure 41: The rectangular beam with a circular cutout, the first segmentation layer on the left, and the second on the right.....	55
Figure 42: The pitched cambered beam, the first segmentation layer on the left, and the second on the right.....	56
Figure 43: Part of the rectangular beam with the circular cutout(a), in comparison with (b) the planned milling paths and (c) the input data of structural analysis. ....	57
Figure 44: Part of the pitched cambered beam (a), in comparison with (b) the planned milling paths and (c) the input data of structural analysis.....	58



Figure 45: Failed cutting on the board's edge. ....	59
Figure 46: Biesse CNC Milling machine, utilizing in OWI GmbH, BIESSE GROUP 2023.....	61
Figure 47: Possible future utilization of this thesis: force-flow oriented segmentations for CNC milling veneer production.....	62

## 9. List of Tables

Table 1: Comparison of input data of two prototypes .....	43
Table 2: Comparison of two segmentation result .....	46